2 of 3

U. S. ARMY
TRANSPORTATION RESEARCH COMMAND
FORT EUSTIS, VIRGINIA

45 of 1.25

TREC TECHNICAL REPORT 61-58

HELICOPTER SHAFT FORCE MEASUREMENT SYSTEM

Task 9R38-13-014-01

Contract DA 44-177-TC-700

April 1961

prepared by:

CORNELL AERONAUTICAL LABORATORY, INC.
Buffalo, New York

(Reprint March 1964)

BLANK PAGE

Project 9R38-13-014-01
Contract DA 44-177-TC-700
April 1961

HELICOPTER SHAFT FORCE MEASUREMENT SYSTEM

Report No TG-1476-F-1

Prepared by:
Cornell Aeronautical Laboratory, Inc.
Buffalo, New York

for
U.S. ARMY TRANSPORTATION RESEARCH COMMAND
FORT EUSTIS, VIRGINIA

Prepared by:
Cornell Aeronautical Laboratory, Inc.
Buffalo, New York

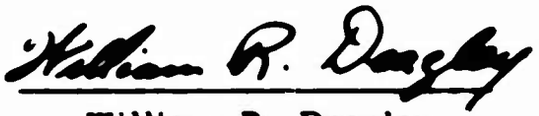

William R. Deasley
CAL Project Engineer

HEADQUARTERS
U. S. ARMY TRANSPORTATION RESEARCH COMMAND
Fort Eustis, Virginia

FOREWORD

The work described in this report has been performed by the Flight Research Department of the Cornell Aeronautical Laboratory, Inc. The program was sponsored by the U. S. Army Transportation Research Command under Contract No. DA 44-177-TC-700. Its purpose was to instrument a HU-1A helicopter in order to measure main rotor shaft horizontal and vertical forces separate from fuselage forces in simulated forward flight in the NASA-Ames Research Center 40 feet by 80 feet wind tunnel. This data is required to determine rotor-pylon-fuselage interference drag effects and to determine rotor and helicopter performance at high tip speeds and high advance rotors.

The project was administered under the direction of the U. S. Army Transportation Research Command, Fort Eustis, Virginia. The report has been reviewed in detail by USATRECOM and the data set forth are concurred with.

FOR THE COMMANDER:

Robert D. Powell Jr.
ROBERT D. POWELL, JR.
USATRECOM, Project Engineer

Earl A. Wirth
EARL A. WIRTH
CWO-4 USA
Adjutant

BLANK PAGE

TABLE OF CONTENTS

LIST OF ILLUSTRATIONS

LIST OF TABLES

LIST OF SYMBOLS

x,y,z	axes in fuselage frame of reference, z axis parallel to rotor shaft axis
H_x	longitudinal shaft shear
H_y	lateral shaft shear
T	shaft tension
θ	instantaneous shaft angle
ϕ	angle of applied force
$H(t)$	force
S_T	stress due to tension
ϵ	strain
I	moment of inertia
M	moments resulting from horizontal shear
C	distance from neutral axis to strained surface

Subscripts

Δ	differential

BLANK PAGE

INTRODUCTION

The development of instrumentation to measure shaft shear and tension forces was undertaken by the Cornell Aeronautical Laboratory, Inc., as a result of a request by the Transportation Research Command (TRECOM) of the Army to aid in the measurement of the rotor shaft forces on an HU-1 Helicopter to be tested in the 40 foot by 80 foot wind tunnel at the NASA Ames Research Center. Similar instrumentation was developed by CAL for use in a helicopter stability derivative measurement program discussed in References 1 through 5.

Since it is not possible to measure the rotor-fuselage interaction forces on the wind tunnel balances, it is necessary to measure the main rotor shaft forces. These forces are the only direct measurement of the interaction between the fuselage and rotor system. Strain gages have been mounted on the rotor shaft to measure directly the strains resulting from shear and tension forces. The three forces which can be measured are the x, y, and z components of the rotor-fuselage interaction.

These forces are called the Longitudinal Shaft Shear (H_x), Lateral Shaft Shear (H_y), and Shaft Tension (T). All measurements are necessarily referenced to the axis of the main rotor shaft.

For ease of computation and data evaluation, it is desirable to obtain an indication of these shaft forces in the fuselage frame of reference rather than the rotating axis system of the rotor. Since the only forces available for direct measurement exist in the rotating shaft, a coordinate transformation is necessary.

To obtain a measurement of shaft forces in the non-rotating axis system, the signals representing shaft forces in the rotating system must be summed in a sine-cosine resolver rotating at shaft speed. This transforms the rotating system data into data in the non-rotating coordinate system. The shaft tension measurement is independent of shaft angle, so no axis transformation is necessary.

DISCUSSION OF H_x, H_y MEASUREMENT SYSTEM

The following is the mathematical basis for the system operation Scale factors and conversions between forces, strains, voltages, and trace deflections are omitted since they only tend to obscure the simple trigonometric operations

Let ϕ be the instantaneous shaft angle ($\phi = 0$ when the reference fixed in the shaft is aligned along the longitudinal axis of the aircraft and to the rear) and θ the angle of the applied force $H(t)$ as shown in the diagram

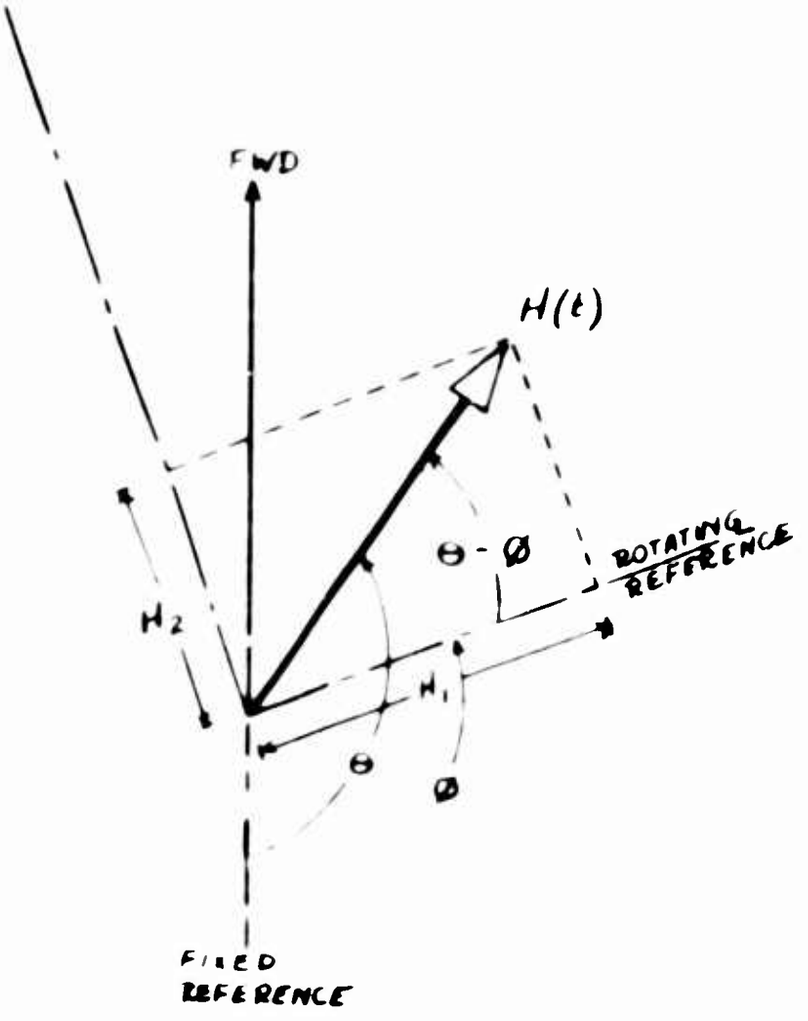

Then the shear forces which would be observed in the two planes at right angles to each other, parallel to the axis of the shaft and fixed with respect to the rotating shaft (i e , the planes coincident with the strain gage locations) are

$$H_1 = H(t)\cos(\Theta - \phi) \qquad (1)$$
$$H_2 = H(t)\sin(\Theta - \phi)$$

These signals are introduced into a sine-cosine resolver which is connected to form the products and sums

$$H_A = H_1 \sin\phi + H_2 \cos\phi$$
$$H_B = H_1 \cos\phi - H_2 \sin\phi \qquad (2)$$

Substituting (1) into (2)

$$H_A = H(t)\sin\phi\cos(\Theta - \phi) + H(t)\cos\phi\sin(\Theta - \phi)$$
$$H_B = H(t)\cos\phi\cos(\Theta - \phi) - H(t)\sin\phi\sin(\Theta - \phi)$$

This reduces to

$$H_A = H(t)\left[\sin(\phi + \Theta - \phi)\right] = H(t)\sin\Theta = H_y$$
$$H_B = H(t)\left[\cos(\Theta - \phi + \phi)\right] = H(t)\cos\Theta = -H_x$$

These equations are independent of ϕ H_x and H_y are the components of shaft shear along the longitudinal and lateral directions

The selection of signs and proper summation is accomplished in practice by reversing the sign of H_1 or H_2 until an input appears to be independent of shaft angle The proper x and y axes are obtained by rotating the resolver case relative to the shaft until the output of H_y is zero when only a H_x input is applied

Figure 1 is a block diagram of the H_x, H_y measurement system:

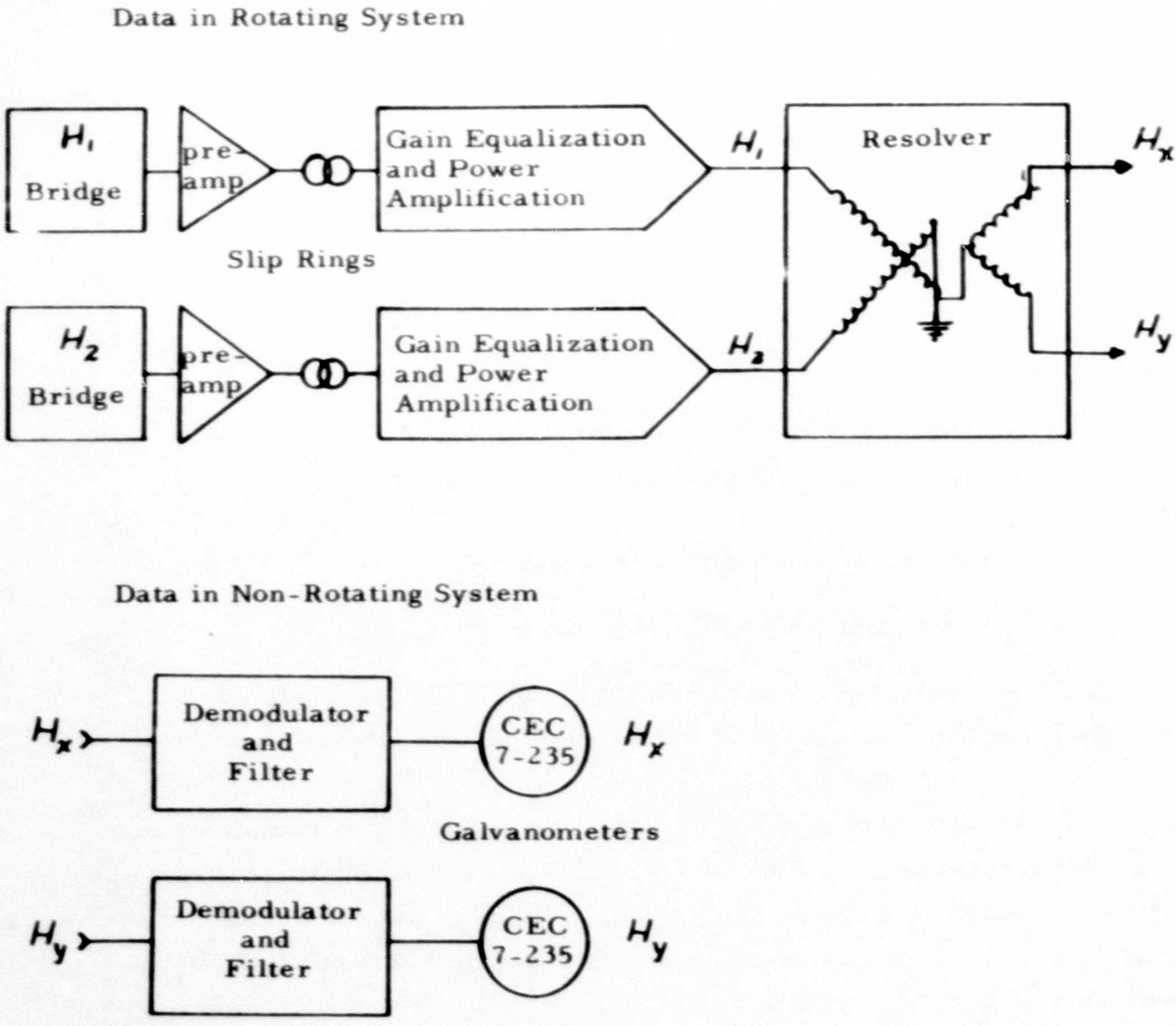

FIGURE 1 BLOCK DIAGRAM OF H_x, H_y MEASUREMENT SYSTEM

ANALYSIS OF ROTOR SHAFT STRAIN AND SIGNAL LEVELS

Tension Measurement

The shaft strain resulting from axial tension is computed, assuming the tensile stresses are uniform around the shaft.

$$\text{Shaft Cross-Section Area} = \pi \left(\frac{3.500^2 - 3.125^2}{4} \right) = 1.95 \text{ in}^2$$

Assume a vertical load of 1000 lb, then the stress due to tension is.

$$S_T = \frac{1000 \text{ lb}}{1.95 \text{ in}^2} = 512.8 \text{ lb/in}^2$$

This is equivalent to 2564.0 lb/in^2 for a 5000 lb load.

$$\text{The strain } \epsilon = \frac{512.8 \text{ lb/in}^2}{30 \times 10^6 \text{ lb/in}^2} = 17.1 \times 10^{-6}/1000 \text{ lb}$$

1 microinch/inch strain is equivalent to 58.5 lb of applied load. A 5000 lb load produces 85.5 microinches/inch strain.

Since the strain gage bridge is a four arm bridge employing tension and Poisson's Ratio compression arms, the effective bridge output is (for gage factor of 2.0).

1.29×10^{-6} volt/volt supply per microinch/inch strain

This becomes

$1.29 \times 10^{-6} \times 26$ volts $\times$ 17.1 volts/1000 lb load = 575×10^{-6} volts per 1000 lb load.

Figure 2 is a signal flow diagram which shows the various forms of the signal through the tension data channel.

From calibration results the hysteresis and repeatability of the data was in the range of 5 to 10 lb for a 5000 lb range of input. This is equivalent to a 2.5 to 5 microvolt uncertainty in the bridge balance.

Full bridge output voltage was 2.87×10^{-3} volts. This was transformed by a factor of 1.55 and preamplified at the rotor by a solid state feedback stabilized amplifier having a gain of 500. The amplifier exhibited a constant gain into the load for output levels up to 7 volts. Since the output for 5000 lb tension was 2.2 volts, no non-linearity or saturation was to be expected.

Because of the necessary decoupling and phase correcting networks, this reduced to approximately 1.5 volts RMS at the demodulator. The resultant current to the recording galvanometer was approximately 36×10^{-6} amperes. The galvanometer sensitivity of 7.9×10^{-6} amperes per inch deflection resulted in a deflection sensitivity of approximately 1110 lb/in. This calculation agrees reasonably well with the 1200 lb/inch calibration factor obtained experimentally.

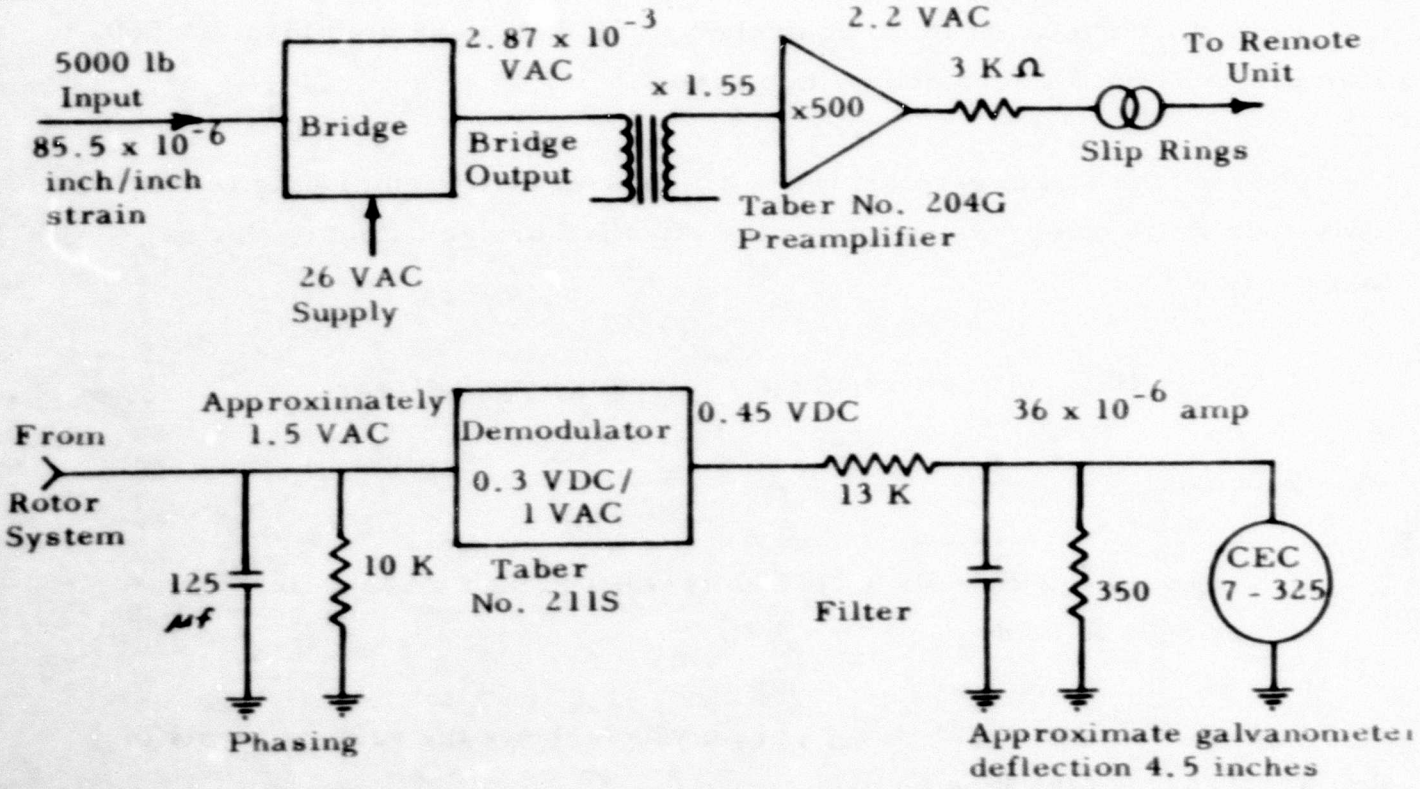

FIGURE 2 TENSION SIGNAL FLOW DIAGRAM

Longitudinal and Lateral Shaft Shear

Strain gages were located at two stations on the main rotor shaft in such a manner that they would sense differential bending moments in the shaft This differential is the result of shear forces at right angles to the shaft axis.

These gages were oriented in two planes intersecting at right angles along the axis of the shaft.* Thus, the instantaneous orthogonal components of shaft shear were obtained in a frame of reference fixed with the shaft.

The strain levels and resultant signal levels were computed in the following manner.

For a hollow cylinder the moment of inertia along one of its diameters is:

$$I = \frac{\pi}{64}(D^4 - d^4) = .0491\,(150 - 95.4) = 2.685 \text{ in}^4$$

the stress $S_\Delta = M_\Delta C/I$ where

M_Δ = differential moments resulting from horizontal shear

= 500 lb shear x 10 inch separation of gage locations**

= 5000 in/lb

C = 1.750 inch

the differential stress

$$S_\Delta = \frac{5000 \times 1.750}{2.685} = 3260 \text{ lb/in}^2 \text{ per } 500 \text{ lb}$$

and the differential strain

$$\epsilon_\Delta = \frac{3260}{30 \times 10^6} = 108.3 \times 10^{-6} \text{ in/in}$$

for a 500 lb shear load.

The resolution and hysteresis limit obtained during calibrations was approximately 1 lb. This is equivalent to 0.2×10^{-6} in/in strain.

---

* See Figure 3, which is a pictorial drawing of the gage installation and a schematic of the bridge interconnections, and Figure 4 is a photograph of a portion of the installation.

** 500 lb is the maximum expected shear load.

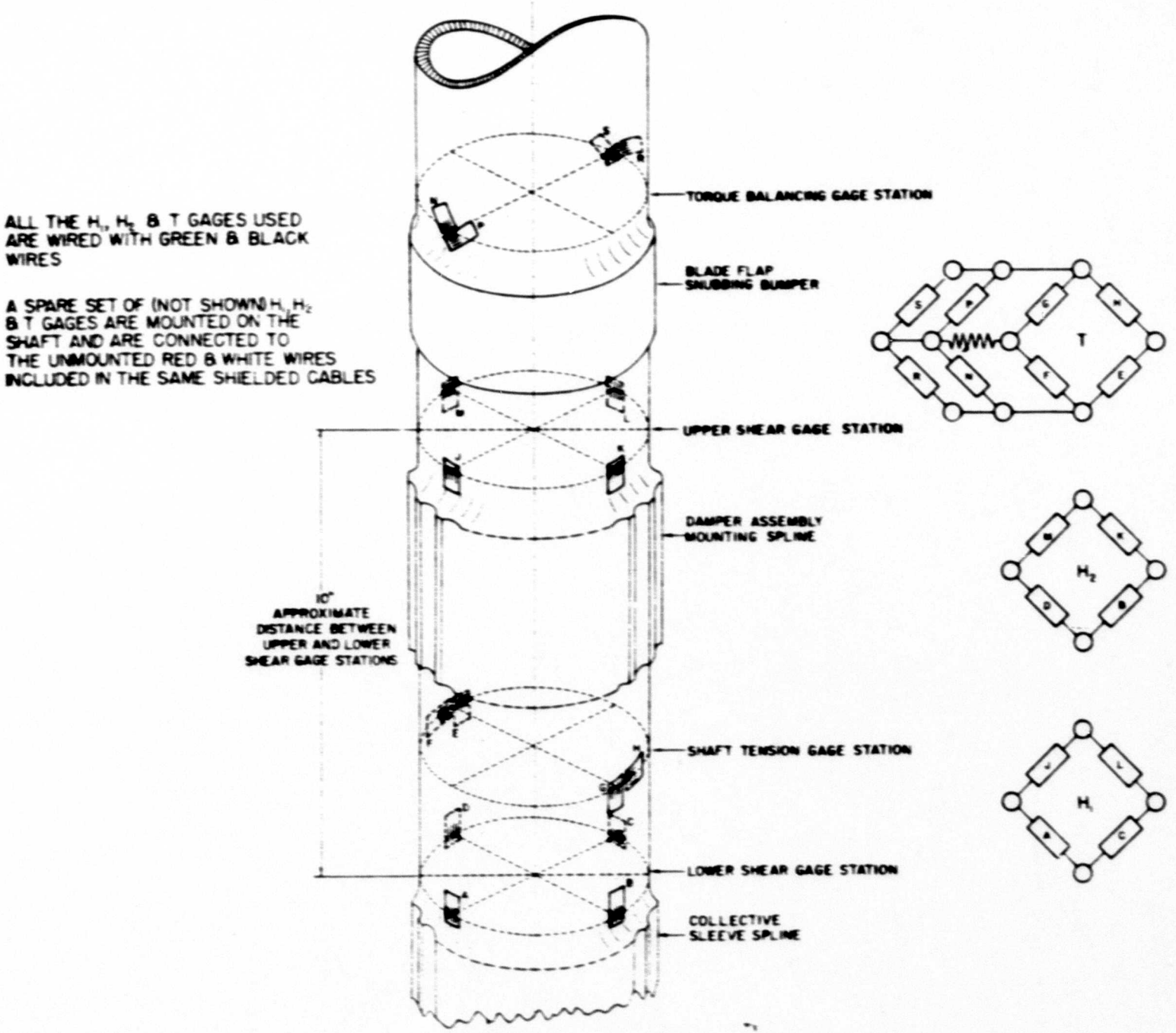

FIGURE 3 PICTORIAL VIEW OF GAGE INSTALLATION

8

TG-1476-F-1

BLANK PAGE

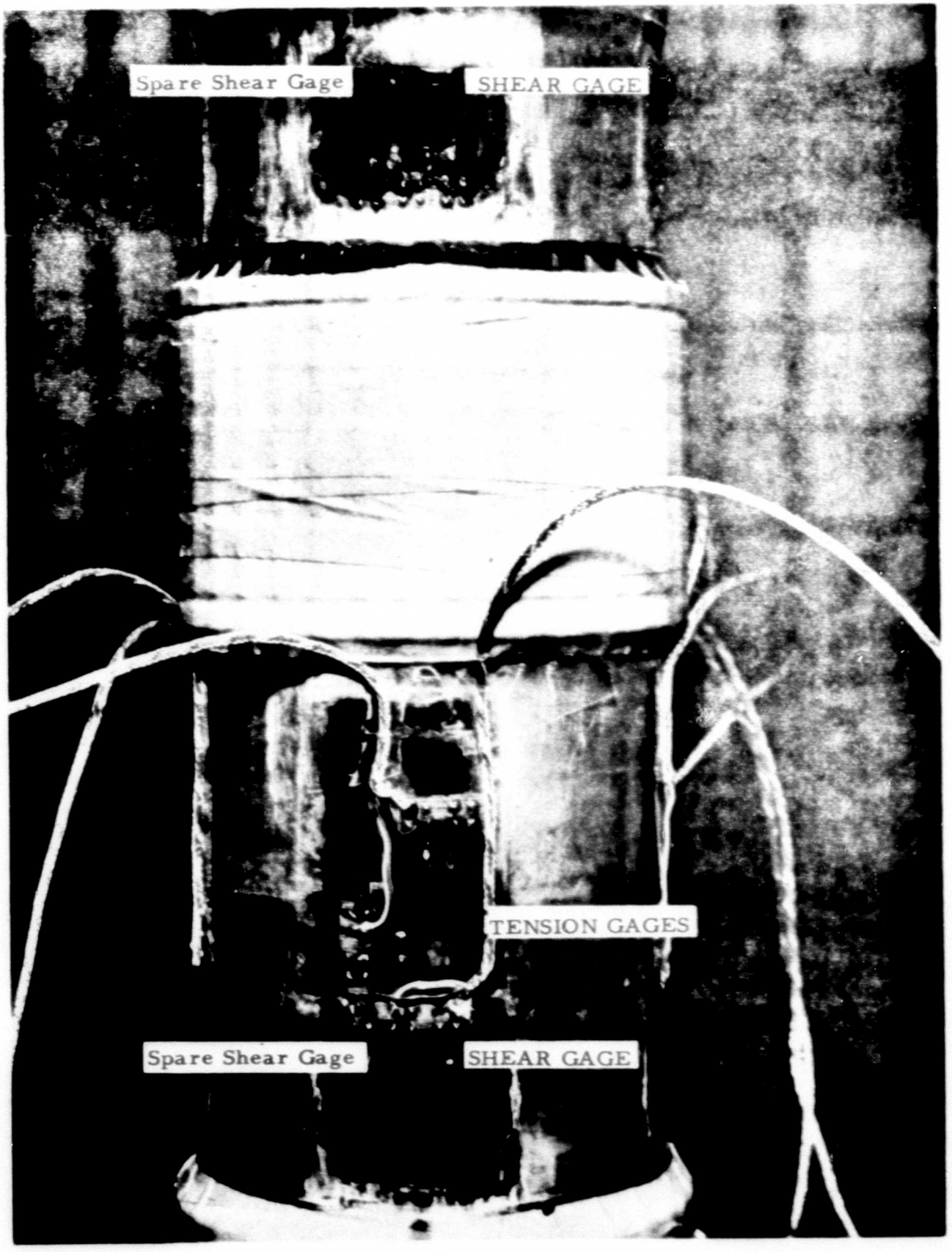

FIGURE 4 PORTION OF GAGE INSTALLATION

Figure 5 is a signal flow diagram showing the various voltage levels through one of the two shear channels.

Assuming a gage supply voltage of 26 VAC and a gage factor of 2, $e_a = 26 \times 2 \times 108.3 \times 10^{-6} = 5.64 \times 10^{-3}$ volts/500 lb. A 1 lb shear load is equivalent to about 12×10^{-6} volts. This is an easily detectable signal.

A 1.55 step-up in an isolation transformer and an amplifier gain of 150 resulted in a full-scale output of the rotor head preamplifiers of $1.55 \times 150 \times 5.64 \times 10^{-3}$ volts = 1.31 volts RMS.

The resultant output voltage of the resolver amplifier is approximately 5.5 VAC. This reduces to approximately 2.15 VAC at the demodulator. The demodulator output is 0.65 VDC which deflects the 7-325 galvanometer about 3.5 inches on the high sensitivity range and 1.65 on the low sensitivity range.

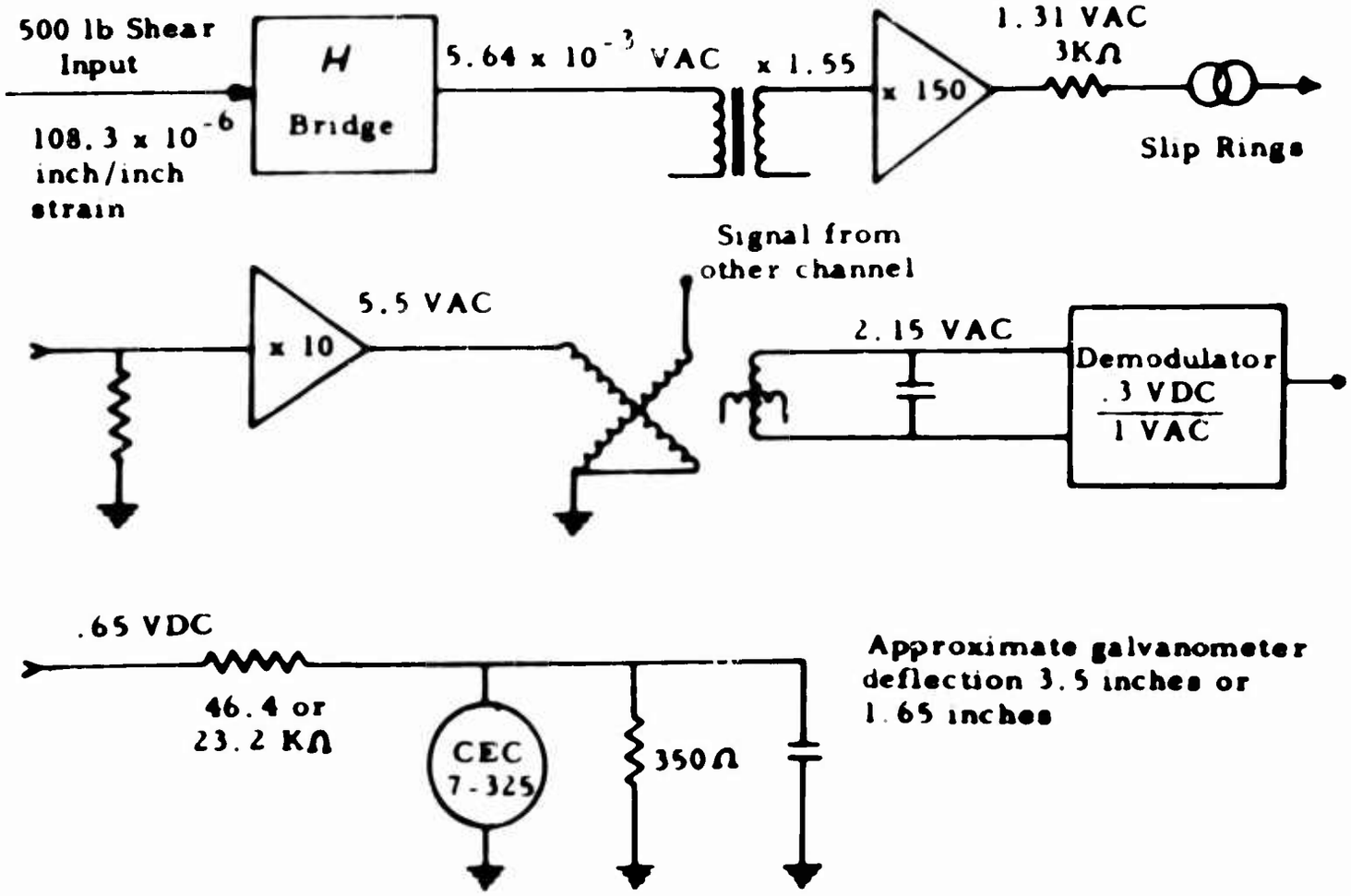

FIGURE 5 SIGNAL FLOW DIAGRAM FOR SHEAR CHANNEL

The mechanization of the measurement system can be separated into four parts

1 Rotor Installation (strain gages and preamplifiers)

2 Remote Test Unit

3 Resolver and Gearbox Installation

4 Recording System

Figure 6 is a block diagram of the complete system and Figures 7, 8, and 9 show in detail the interconnections and circuits of the four sections

The strain gages used for the rotor installation are Tatnal Type C6-141-350 These are 350 ohm metal film strain gages having a gage fac of 2 03 ±1/2% These gages are bonded to the rotor shaft with Eastman 910 cement and waterproofed and protected from injury by a synthetic rubber over coat and fiberglass tape

A duplicate set of strain gages for shear and tension measurements was also installed in the event of a failure of the first set Wiring has been provided so that switching from one set to the other is not difficult Realignment of the resolver would be necessary for the shear channels if this change is made

The strain gage outputs are balanced and amplified by the Rotor Pre amplifier and Balance Unit which is mounted on the damper mounting assembly Bell Part No 204 010 917 1 The resulting signals are transmitted through the slip ring assembly (provided by Bell) and approximately 120 feet of shielded cable to the Remote Test Unit Figure 10 is a photograph of this assembly

The Remote Test Unit consists of two chassis mounted in a cabinet rack The lower unit is a regulated 400 cps supply for the instrumentation and the upper is the chassis which provides the gain controls, test or calibration voltage, power amplification, demodulation and filtering necessary for obtaining M_x, M_y and T

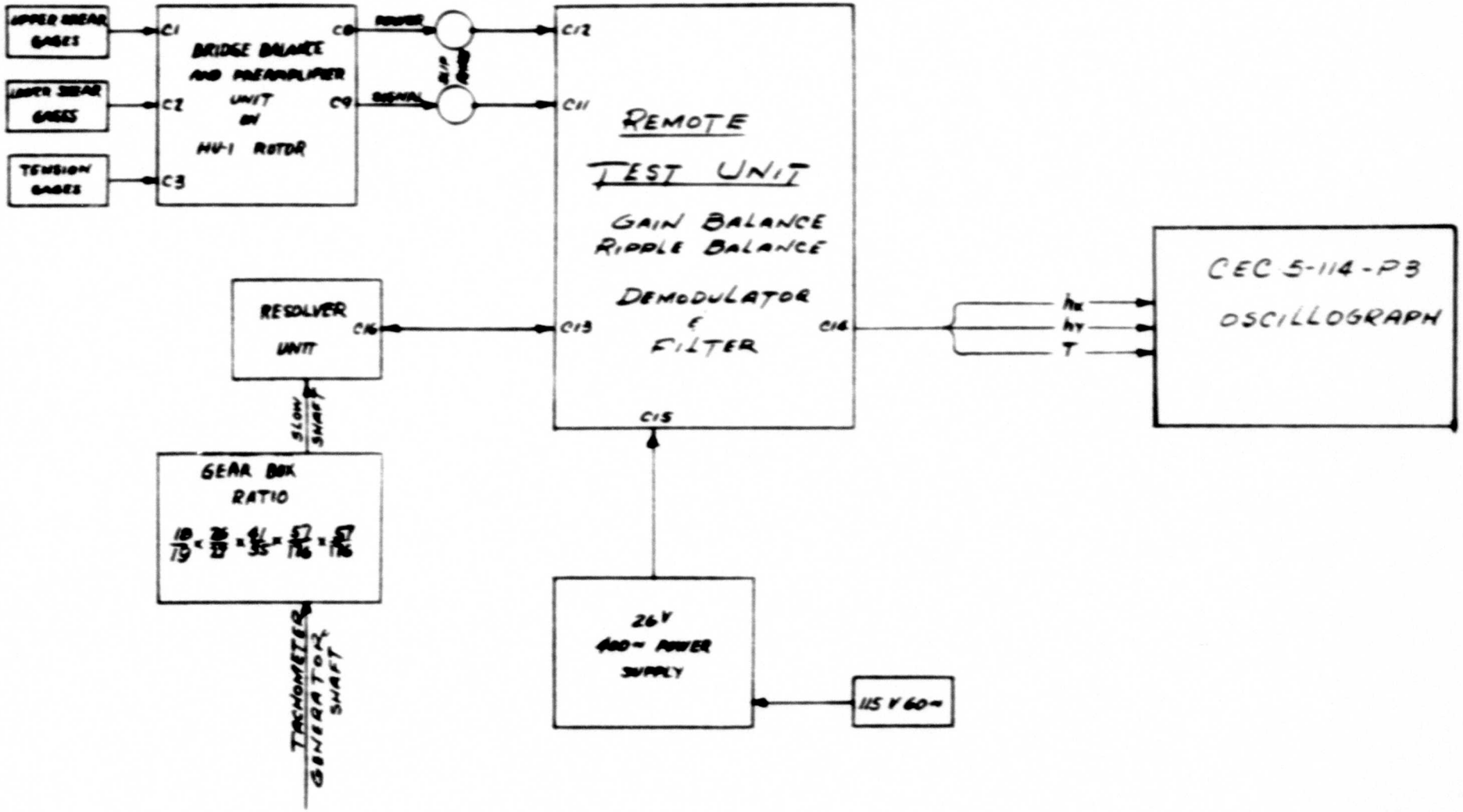

FIGURE 6 BLOCK DIAGRAM OF MEASUREMENT SYSTEM

TG-1476-F-1

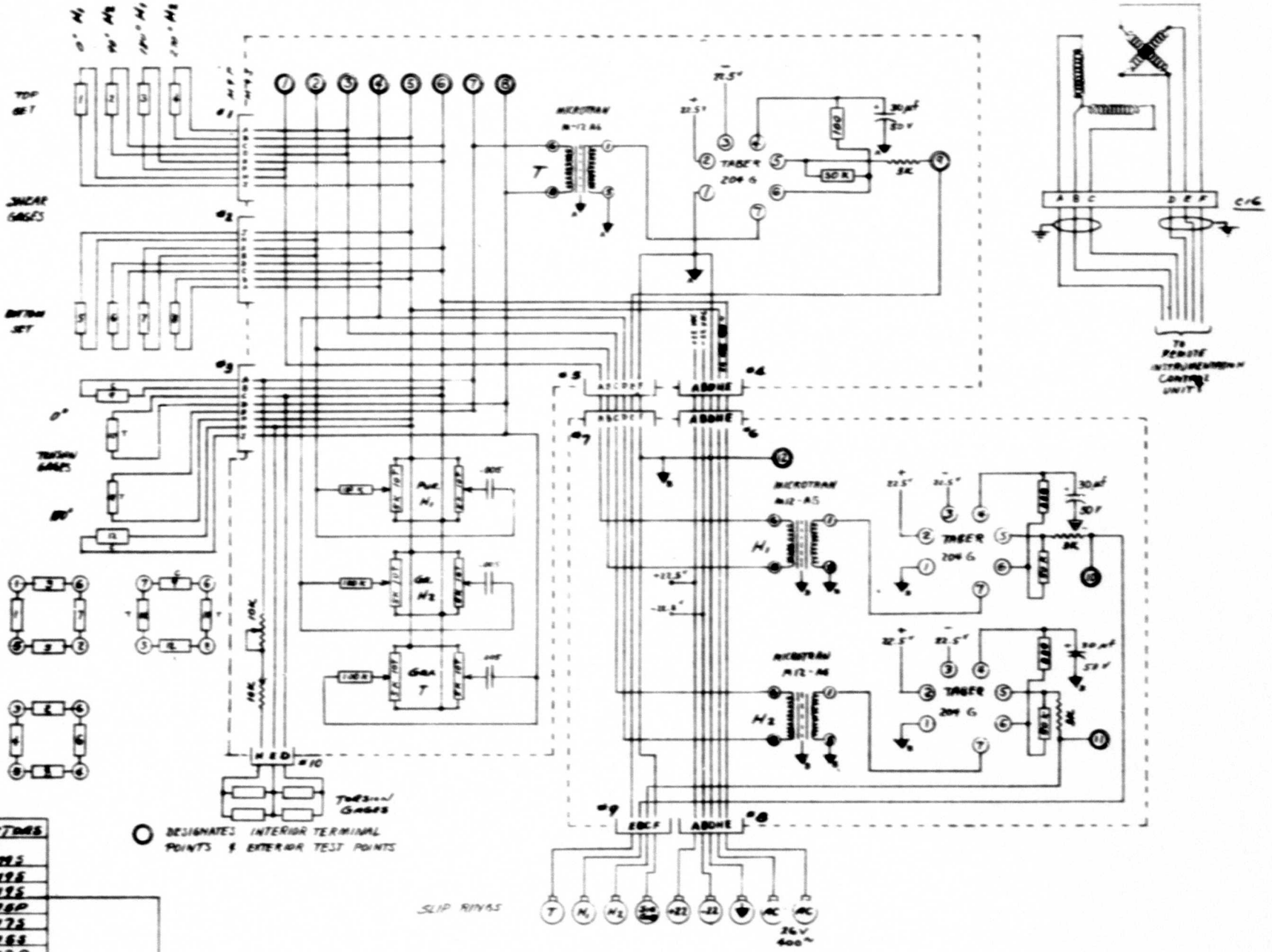

TG-1476-F-1

FIGURE 7 SCHEMATIC OF ROTOR HEAD AND RESOLVER UNITS

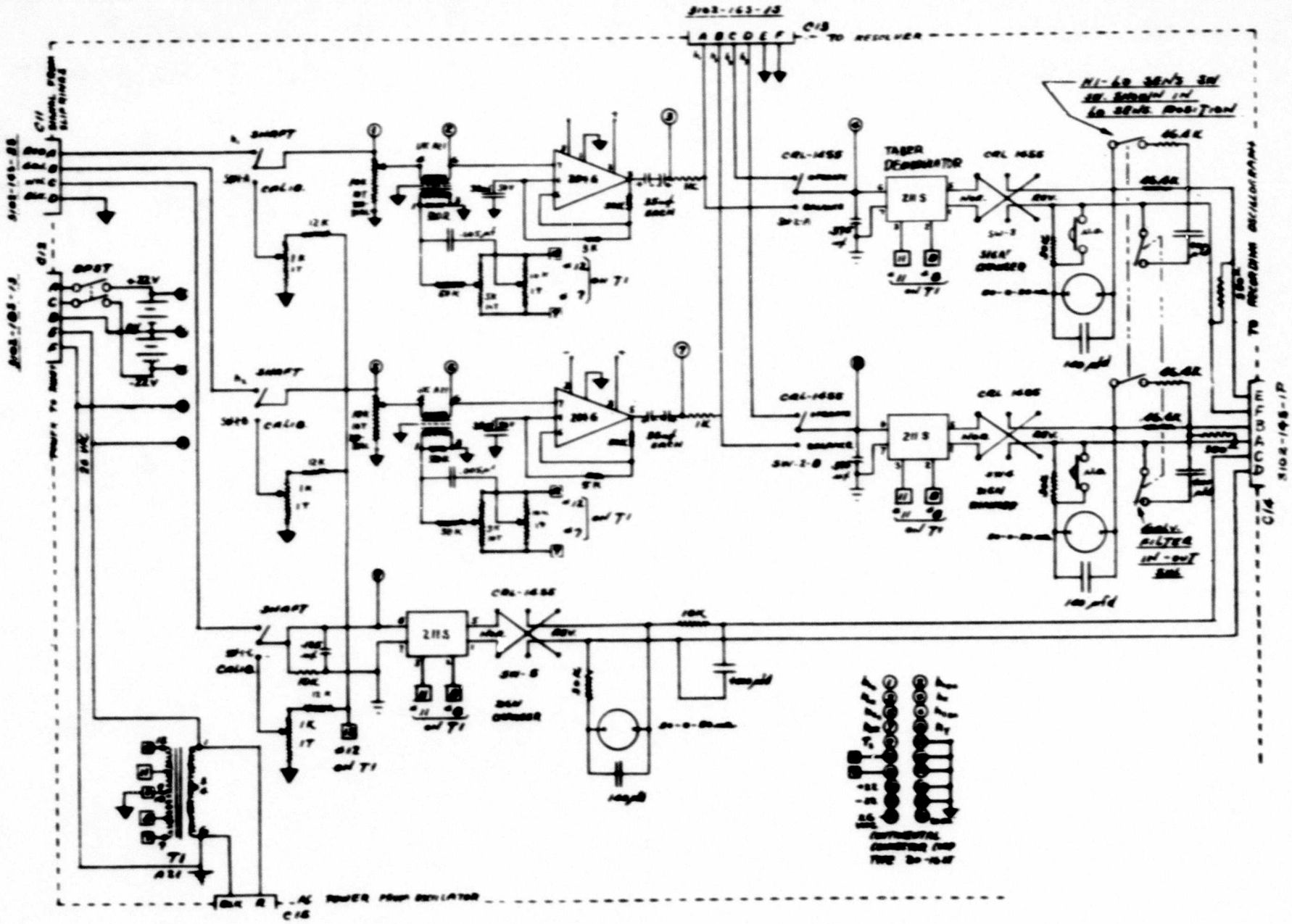

FIGURE 8 SCHEMATIC OF REMOTE TEST UNIT

TG-1476-F-1

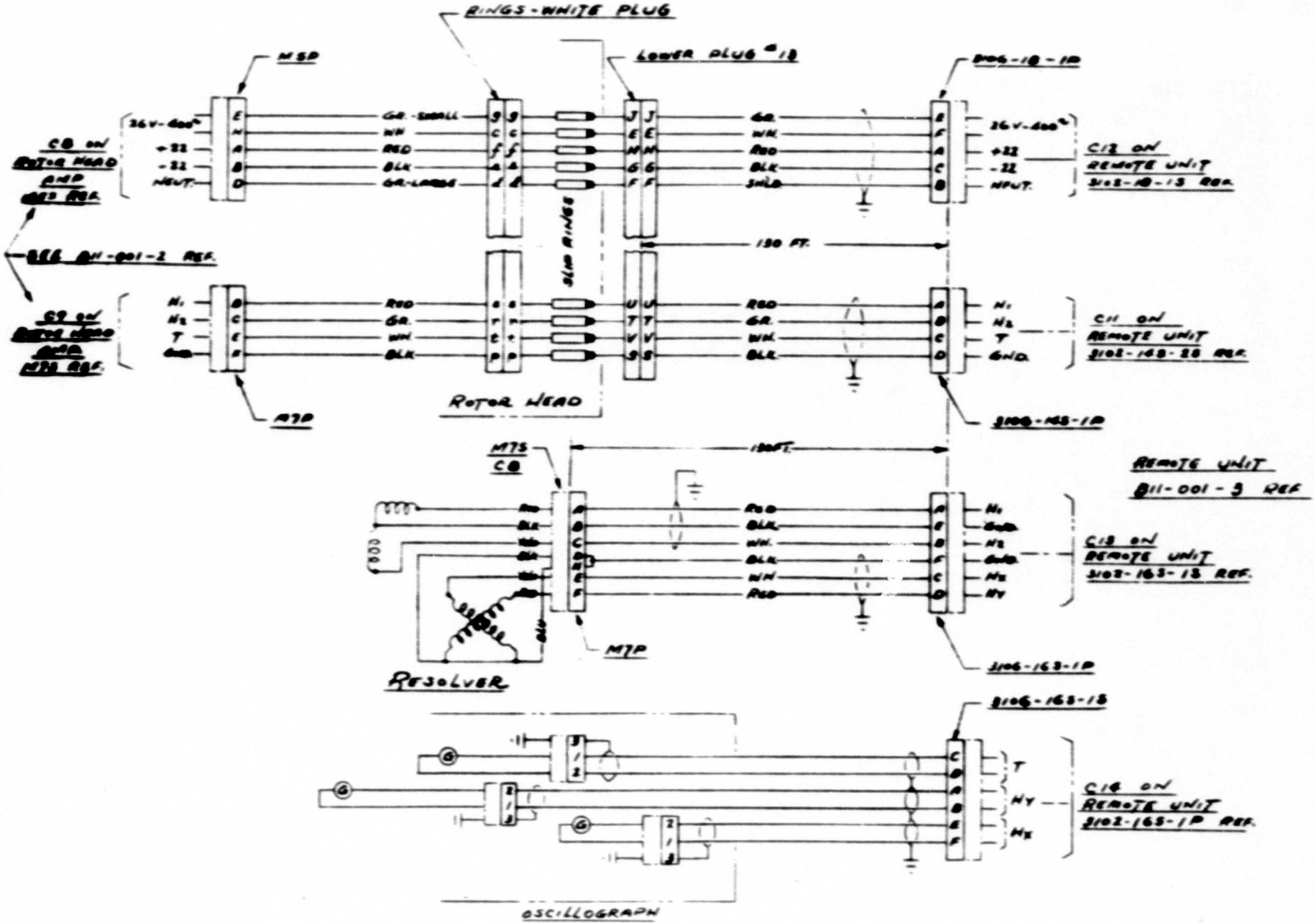

FIGURE 9 INTERCONNECTING CABLES SCHEMATICS

TG-1476-F-1

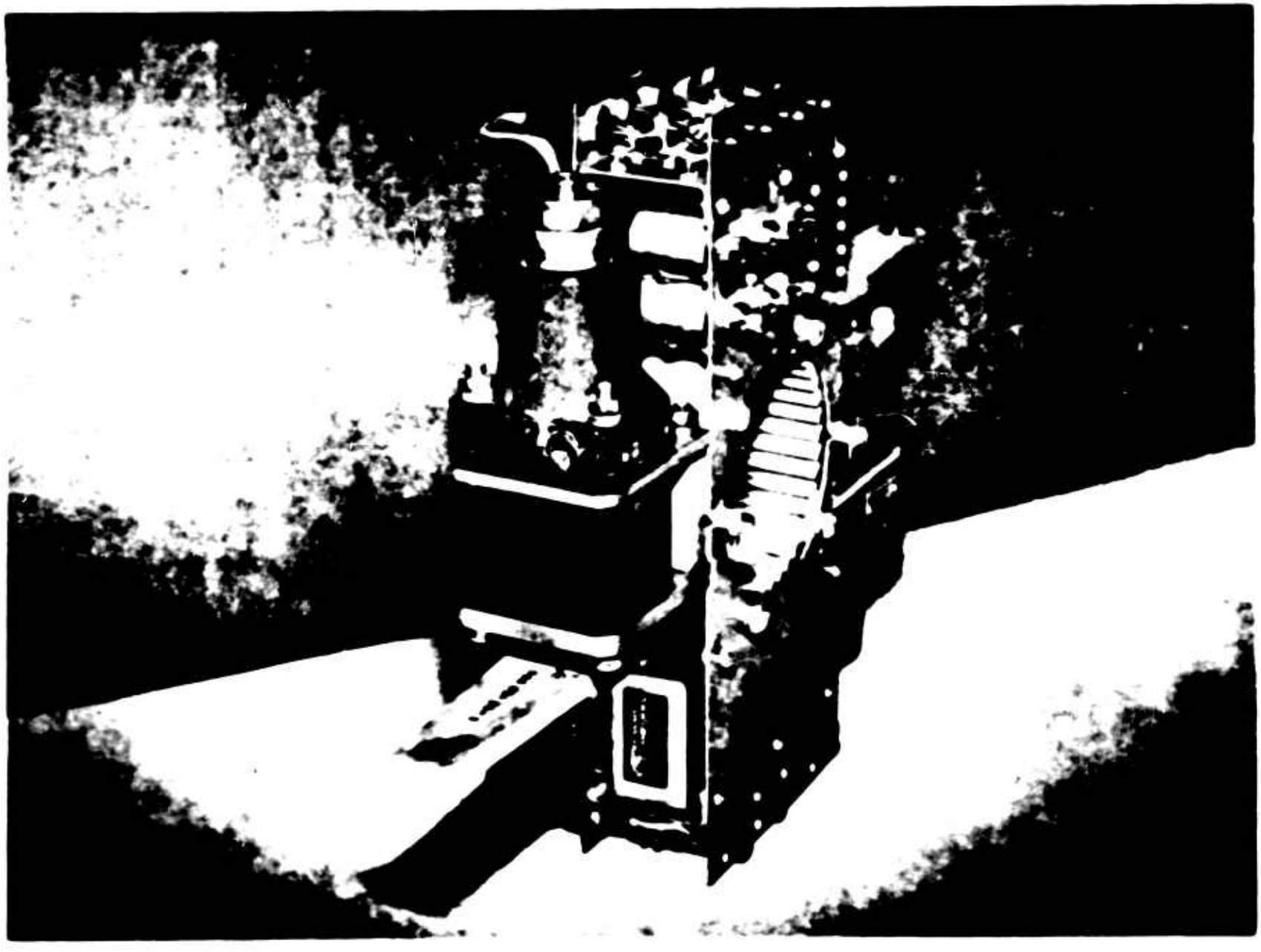

FIGURE 10 ROTOR PREAMPLIFIER AND BALANCE UNIT

TG-1476-F-1

BLANK PAGE

Panel mounted 50-0-50 micro ampere meters are provided for easy visual monitoring of the galvanometer signals and for balancing

The resolver system is mounted on the tachometer generator pad at the lower right side of the main gearbox. Due to structural member interference, it was necessary to rotate the hydraulic pump (and the necessary drain fittings, etc.) 90° to accommodate the gearbox without additional machining. Appendix I is a description of the gearbox.

CALIBRATION PROCEDURES AND RESULTS

Tension

The tension calibration was accomplished by lifting the helicopter by the main rotor and cap which has a lifting eye. A NASA 10,000 lb range proving ring having a calibration factor of 22.8 lb/division was used as a measure of the tension input. The shaft axis was inclined forward about 3 degrees. This would result in a 0.275% reduction in the tension along the axis.

Calibrations were made for every 90° position of the shaft. A noticeable difference in the deflection sensitivity was obtained for the various azimuth positions. Since this was discovered to be mainly due to bending moment cross talk in the extra pair of gages used for nulling the torsion cross talk, a similar pair of gages was mounted at an azimuth position of 180° from the original pair. These gages will reduce the effects of bending moments to a negligible amount.

The calibrations presented here were made with only the two original torsion nulling gages. This shows up as an increase and decrease in deflection sensitivity with shaft azimuth position. It was not possible to lift the helicopter with the slip rings installed since the blade assembly was removed. These calibrations were made without the possible small effect of slip rings. The 3000 ohm series resistor in the preamplifier output should make the effect of the rings negligible.

The average of the four calibrations is very near the deflection sensitivity of the system with no bending moment inputs. This average was obtained by taking the average of the trace deflections for each value of tension load. Since a few of the tension loads did not agree exactly with the nominal value, small correction factors (of the order of .02 inches) were introduced to simplify the averaging procedure.

Table I presents the input tension and resultant trace position for the four azimuth positions. Table II tabulates the corrected deflections for the nominal tension inputs listed and the resultant linear average of the four calibrations. One point for the 180° azimuth position was off-scale. This point was obtained by extrapolation since it was important for a consistent method of averaging. The resulting calibration is shown in Figure 9. The non-linearity between zero and 1000 lb resulted from the rest position of the galvanometer being offset beyond its linear range. This is not important since the data will all be obtained in the 4000 to 6000 range of loads.

The hysteresis of the averaged calibration was not reduced appreciably by the averaging technique. The resulting maximum hysteresis is about .03 in. This is equivalent to about 34 lb hysteresis or 34/5000 x 100% = 0.7% of full scale.

The data obtained from the tension channel during wind tunnel tests will not be as accurate as was obtained during the calibrations because of the temperature drifts, torque cross talk, vibration and noise resulting from the captive flights. Filtering is provided which will aid greatly in averaging out the noise, but it will be necessary to establish a reference value of tension after a warm-up period. During flight, the rotor shaft temperature rises and it is desirable to establish the 5000 lb point at test operating temperature. The calibration factor will also be changed due to the variation of Young's Modulus with temperature. This is of the order of -1% for each 30° C rise. This correction can be applied to the test data by checking the shaft temperature just after shutdown.

Shaft Shear

The calibration of the shaft shear channels was preceded by a sequence of adjustments necessary for the initial setting up of the measurement system.

In Equation 2 an incorrect sign in either H_1 , H_2 , or in the method of summing these signals in the resolver will result in

TABLE I

INPUT TENSION AND RESULTANT TRACE POSITION

Azimuth 0°		Azimuth 90°		Azimuth 180°		Azimuth 270°	
Lb Load	Trace Deflection	Lb Load	Trace Deflection	Lb Load	Trace Deflection	Lb Load	Trace Deflection
0	-0.10	0	-0.11	0	-0.11	0	-0.22
1140	+1.03	1133	+1.01	1140	+1.07	1140	+0.95
2280	2.03	2285	2.05	2280	2.11	2280	1.96
3420	3.00	3420	2.99	3420	3.13	3420	2.98
4560	3.98	4610	4.01	4560	4.17	4560	4.00
5110	4.45	5080	4.43	5100	4.66*	5130	4.55
4560	4.00	4560	4.00	4560	4.15	4560	4.00
3420	3.01	3445	3.03	3420	3.12	3420	3.00
2280	2.05	2280	2.04	2290	2.11	2280	2.00
1140	+1.05	1140	+1.05	1150	+1.09	1140	+0.99
0	-0.12	0	-0.09	0	-0.10	0	-0.18

* extrapolated from 180° calibration curve

TABLE II

CORRECTED DEFLECTION FOR INPUT TENSIONS AND RESULTANT AVERAGE DEFLECTION

NOMINAL WEIGHT	0° Azimuth			90° Azimuth			180° Azimuth			270° Azimuth			AVERAGE DEFLECTION
	Actual Weight lb	Required Correction lb	Corrected Deflection	Actual Weight lb	Required Correction lb	Corrected Deflection	Actual Weight lb	Required Correction lb	Corrected Deflection	Actual Weight lb	Required Correction lb	Corrected Deflection	
0	0	0	-0.10	0	0	-0.11	0	0	-.11	0	0	-0.22	-.135
1140	1140	0	+1.03	1133	+7	+1.02	1140	0	+1.07	1140	0	+0.95	+1.017
2280	2280	0	2.03	2285	-5	2.05	2280	0	2.11	2280	0	1.96	2.036
3420	3420	0	3.00	3420	0	2.99	3420	0	3.13	3420	0	2.98	3.025
4560	4560	0	3.98	4610	-50	3.97	4560	0	4.17	4560	0	4.00	4.029
5100	5110	-10	4.44	5080	+20	4.45	5100	0	4.66	5130	-30	4.52	4.518
4560	4560	0	4.00	4560	0	4.00	4560	0	4.15	4560	0	4.00	4.038
3420	3420	0	3.01	3445	-25	3.01	3420	0	3.12	3420	0	3.00	3.035
2280	2280	0	2.05	2280	0	2.04	2290	-10	2.10	2280	0	2.00	2.058
1140	1140	0	+1.05	1140	0	+1.05	1150	-10	+1.08	1140	0	+0.99	1.043
0	0	0	-0.12	0	0	-0.09	0	0	-0.10	0	0	-0.18	-0.123

correction of .00087 in/lb

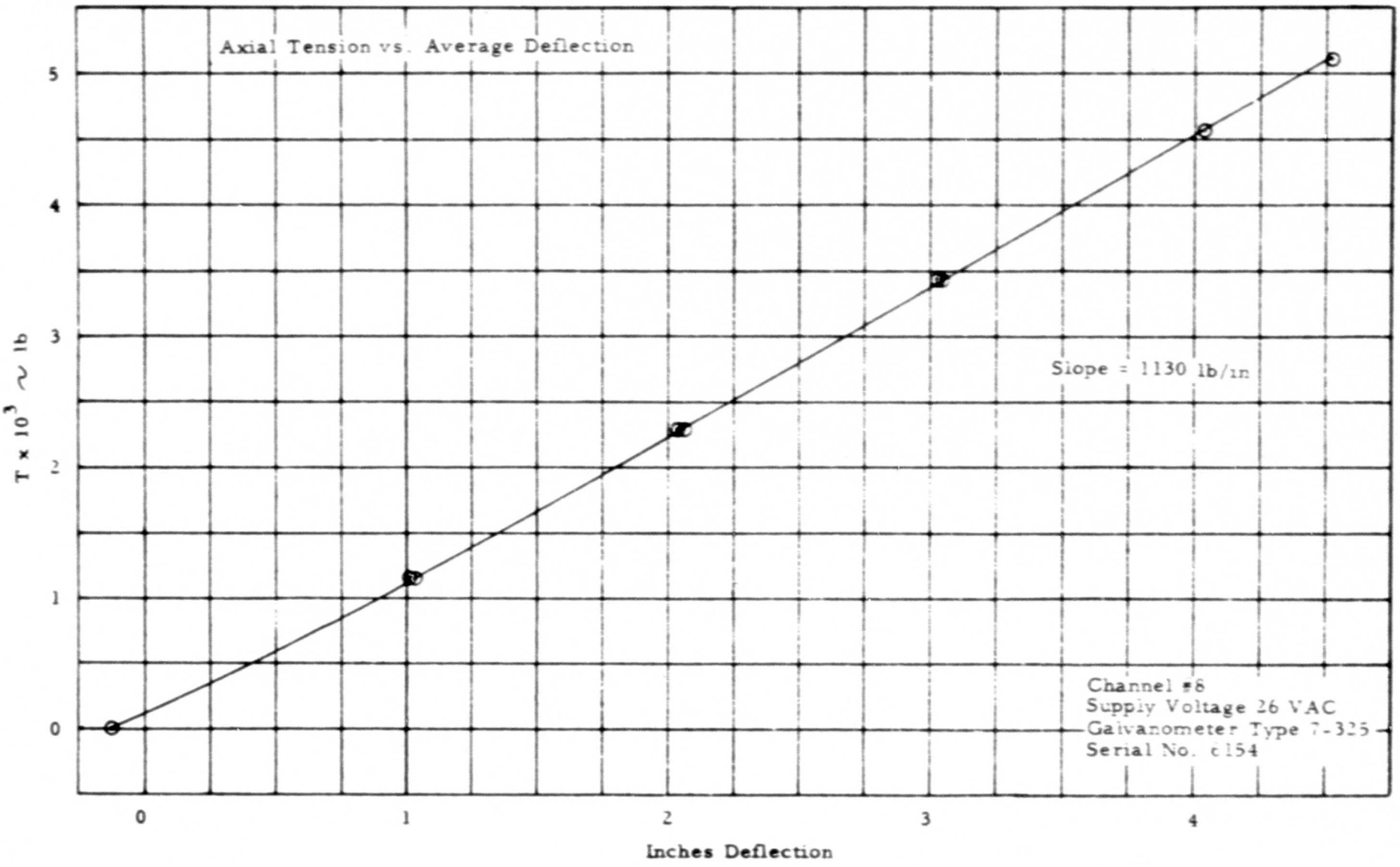

FIGURE 11 SHAFT TENSION CALIBRATION

TG-1476-F-1

BLANK PAGE

$$H_A = H_1 \sin\phi - H_2 \cos\phi$$

$$H_B = H_1 \cos\phi + H_2 \sin\phi$$

expanding,

$$H_A = H(t) \sin\phi \cos(\theta-\phi) - H(t) \cos\phi \sin(\theta-\phi)$$

$$H_B = H(t) \cos\phi \cos(\theta-\phi) + H(t) \sin\phi \sin(\theta-\phi)$$

This reduces to

$$H_A = H(t)\left[\sin(\phi+\theta+\phi)\right] = H(t) \sin(2\phi+\theta)$$

$$H_B = H(t)\left[\cos(\theta-\phi-\phi)\right] = H(t) \cos(\theta-2\phi)$$

These equations are dependent on ϕ and the output is a second harmonic of shaft RPM for a steady input.

By a reversal of either the sign of H_1 or H_2, this second harmonic disappears and the output is a constant.

The output is a constant if the H_1 and H_2 channel gains are equal. If they are not, Equation 1 is changed to:

$$H_1 = H(t)(1+\Delta)\cos(\theta-\phi)$$

$$H_2 = H(t)(1-\Delta)\sin(\theta-\phi)$$

Resolving H_1 and H_2 into the H_A component:

$$H_A = H(t)(1+\Delta)\sin\phi\cos(\theta-\phi) + H(t)(1-\Delta)\cos\phi\sin(\theta-\phi)$$

$$= H(t)\sin\theta + \Delta H(t)\sin(2\phi+\theta)$$

The second term is a 2/rev ripple superimposed on the correct output which results from unequal channel gain. The average gain is unchanged. In the present system, the ripple frequency is approximately 10 cps. The filter has a cut-off at 1 cps so the ripple due to unequal gain is negligible. If there is a static unbalance in H_1 or H_2 due to either bridge unbalance, blade unbalance or tracking errors, this term will appear at the output of the resolver as a function of $\sin\phi$ or $\cos\phi$ (i.e., a 1/rev ripple).

The Remote Balance Unit has provisions for detecting the steady state

unbalance at the input to the resolvers so that this unwanted 1/rev ripple can be reduced to negligible amounts. There is no inherent way to balance out higher order errors without rotating resolvers at multiples of blade RPM.

The orientation of the resolved output is determined by the relative position of the resolver stator and its mounting pad, providing the resolver rotor is rigidly connected to the main rotor shaft or through a 1:1 gearing arrangement. *

The most significant feature of this measurement system is that the steady state output of the H_x or H_y channel can only result from a corresponding steady state input shear on the rotor shaft. Electrical unbalance, mechanical or aerodynamic unbalances will not materially change the steady state deflection. The zero shear balance point can be determined quite accurately by switching off the resolver output or by reversing its sign and noting the average. This zero can be obtained when the rotor is spinning or when it is not turning. The zero current position of the galvanometer could be a false zero if any unbalance exists in the demodulator and, for this reason, should not be used.

The H_x and H_y channels were calibrated for each 45° azimuth position of the rotor shaft. This provided one with sufficient data to establish the average sensitivity of the particular channel.

Some variation in sensitivity for the various shaft positions was observed. The sensitivities in the plane of the strain gage bridges were adjusted to be nearly equal, but the stiffness of the shaft was not constant with azimuth position. This is most likely the result of slight errors in the concentricity of the inner and outer surfaces of the shaft.

---

* See Appendix I for details of the Resolver Gearbox.

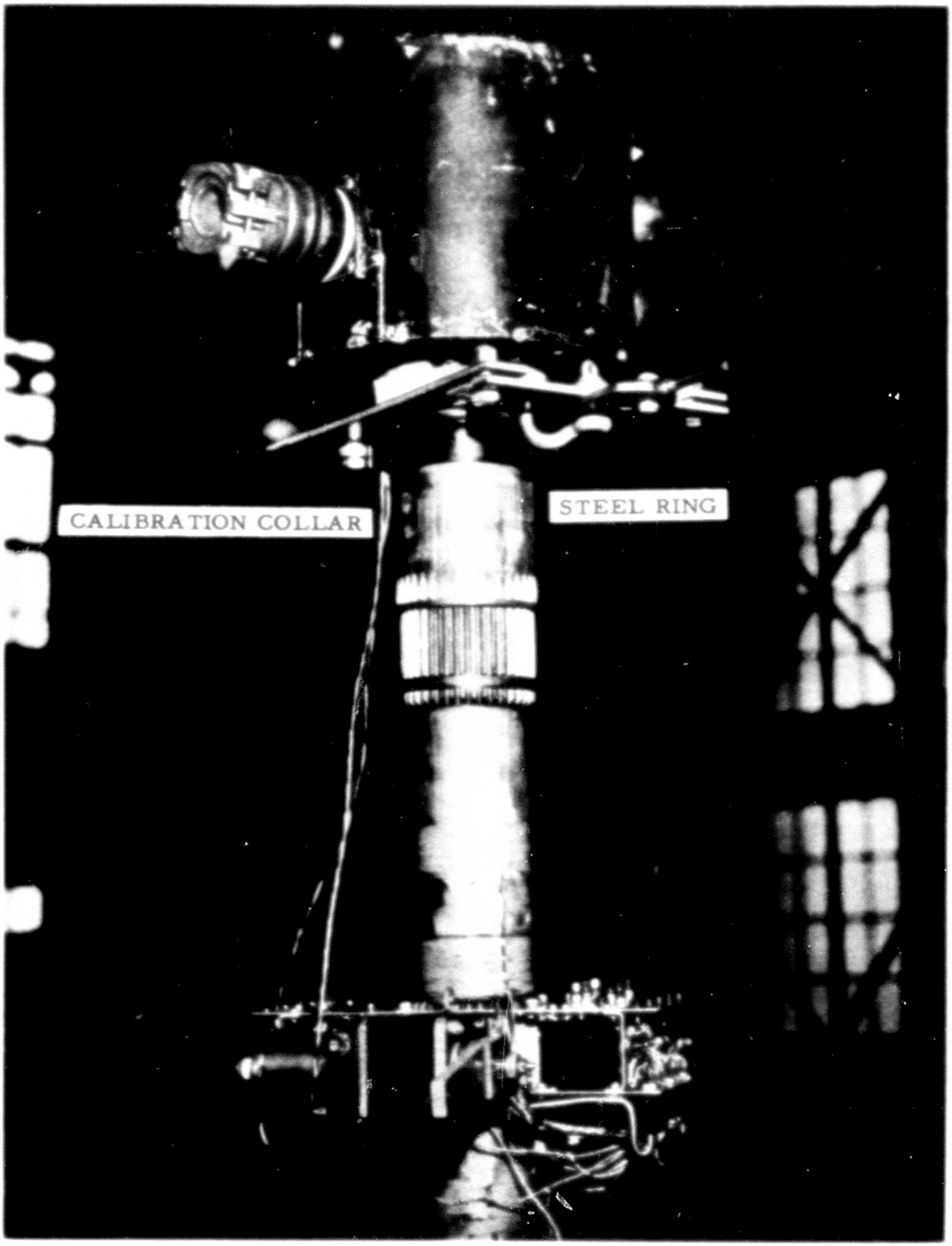

FIGURE 12 SHEAR LOADING FIXTURE

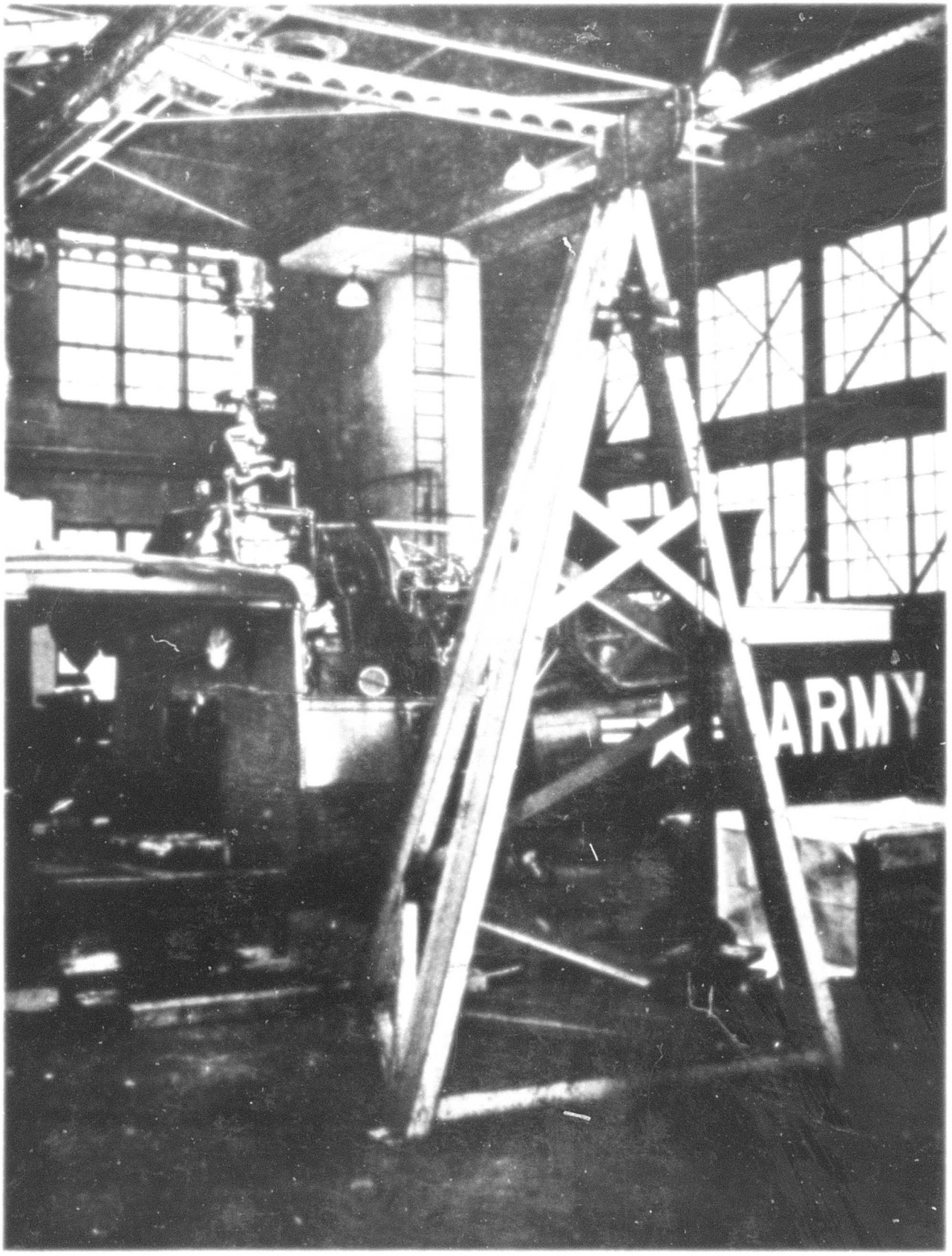

FIGURE 13 CALIBRATION SET-UP FOR H_y CHANNEL

This unequal sensitivity with azimuth position will result in a 2/rev ripple superimposed on the desired deflection. The filtering of the recording channels is sufficient to reduce this to negligible amounts.

Calibrations were performed by applying loads at right angles to the rotor shaft axis in the longitudinal and lateral directions. A steel ring mounted on the shaft and a U-shaped collar with two radial ball bearings bolted to the collar were required as calibration accessories. These were constructed in such a fashion that loads applied from a cable attached to the U-shaped collar were transferred to the radial bearings, which in turn contacted the steel ring without interfering with electrical cables to the Slip Ring Assembly. Thus, it was possible to rotate the rotor shaft without removing the calibration fixture or any load that was applied.

Figure 12 is a photograph of this fixture and Figure 13 is a photograph of the calibration technique used for the H_y calibration.

Loads were applied in 50 lb increments and the channel gains were switched from high to low for each load value. The resultant trace deflections are presented in Tables III and IV.

The average for each load value at both high and low sensitivity settings is presented in Table V.

Figures 14 and 15 are plots of the resulting calibrations.

The linearity and hysteresis errors are less than 1/2% of full-scale.

Figures 16 and 17 are polar plots of the calibration factors for H_x and H_y versus azimuth position. This series of plots is included to show graphically the variation of system sensitivity with angular position.

TABLE III

RESULTANT TRACE DEFLECTIONS FOR HIGH AND LOW H_x CHANNEL GAINS

H_x	0° Azimuth		45° Azimuth		90° Azimuth		135° Azimuth		180° Azimuth		215° Azimuth		270° Azimuth		315° Azimuth	
	High*	Low	High	Low	High	Low	High	Low	High	Low	High	Low	High	Low	High	Low
0	0.62	0.62	0.67	0.71	0.79	0.95	0.62	0.62	0.67	0.71	0.64	0.65	0.62	0.62	0.66	0.69
50	0.85	1.07	0.90	1.16	1.03	1.41	0.86	1.09	0.90	1.15	0.86	1.09	0.86	1.08	0.90	1.16
100	1.08	1.51	1.13	1.61	1.26	1.88	1.10	1.55	1.12	1.60	1.09	1.54	1.10	1.55	1.13	1.62
150	1.31	1.95	1.35	2.04	1.50	2.33	1.34	2.01	1.35	2.04	1.31	1.97	1.33	2.00	1.36	2.07
200	1.53	2.39	1.58	2.48	1.73	2.78	1.56	2.46	1.57	2.48	1.54	2.40	1.57	2.46	1.60	2.52
250	1.75	2.84	1.80	2.91	1.96	3.23	1.80	2.92	1.79	2.91	1.76	2.84	1.80	2.92	1.82	2.97
300	1.97	3.25	2.01	3.34	2.18	3.68	2.02	3.37	2.01	3.34	1.97	3.26	2.02	3.36	2.05	3.42
350	2.18	3.68	2.23	3.76	2.41	4.13	2.25	3.81	2.23	3.78	2.18	3.68	2.24	3.80	2.27	3.87
400	2.40	4.11	2.44	4.19	2.63	4.56	2.48	4.26	2.45	4.20	2.40	4.10	2.47	4.25	2.50	4.31
450	2.61	4.53	2.66	--	2.86	--	2.69	--	2.65	--	2.62	4.54	2.70	--	2.73	--
500	2.83	--	2.86	--	3.08	--	2.92	--	2.88	--	2.83	--	2.91	--	2.95	--
450	2.62	4.54	2.66	--	2.86	--	2.71	--	2.64	--	2.63	4.56	2.71	--	2.74	--
400	2.40	4.12	2.45	4.22	2.64	4.58	2.49	4.28	2.45	4.22	2.41	4.13	2.48	4.27	2.52	4.34
350	2.19	3.69	2.24	3.79	2.42	4.14	2.26	3.83	2.24	3.80	2.19	3.70	2.25	3.82	2.29	3.90
300	1.97	3.26	2.02	3.36	2.19	3.70	2.03	3.38	2.02	3.35	1.98	3.27	2.03	3.38	2.06	3.44
250	1.75	2.83	1.80	2.93	1.97	3.25	1.80	2.93	1.80	2.92	1.76	2.84	1.81	2.93	1.84	3.00
200	1.54	2.40	1.59	2.50	1.73	2.80	1.57	2.49	1.78	2.50	1.54	2.40	1.57	2.48	1.61	2.54
150	1.31	1.96	1.36	2.06	1.51	2.34	1.34	2.02	1.36	2.05	1.32	1.97	1.34	2.02	1.38	2.09
100	1.09	1.53	1.14	1.62	1.27	1.88	1.10	1.56	1.13	1.61	1.09	1.53	1.10	1.56	1.14	1.63
50	0.86	1.08	0.91	1.18	1.03	1.42	0.87	1.10	0.90	1.16	0.86	1.09	0.87	1.09	0.91	1.17
0	0.63	0.63	0.68	0.73	0.79	0.95	0.63	0.63	0.67	0.71	0.63	0.63	0.62	0.62	0.66	0.70

*Highs and lows in inches of deflection

TABLE IV

RESULTANT TRACE DEFLECTIONS FOR HIGH AND LOW H_y CHANNEL GAINS

H_y	0° Azimuth		45° Azimuth		90° Azimuth		135° Azimuth		180° Azimuth		225° Azimuth		270° Azimuth		315° Azimuth	
lb	High*	Low	High	Low	High	Low	High	Low	High	Low	High	Low	High	Low	High	Low
0	0.78	0.75	0.79	0.79	0.84	0.85	0.80	0.81	0.81	0.82	0.82	0.82	0.81	0.81	0.80	0.79
50	1.01	1.20	1.01	1.21	1.05	1.28	1.02	1.23	1.04	1.26	1.05	1.27	1.03	1.23	1.02	1.23
100	1.23	1.65	1.25	1.66	1.27	1.71	1.24	1.66	1.27	1.69	1.27	1.70	1.24	1.65	1.24	1.65
150	1.46	2.10	1.46	2.09	1.49	2.13	1.47	2.10	1.48	2.13	1.49	2.14	1.46	2.08	1.46	2.09
200	1.69	2.53	1.69	2.53	1.70	2.55	1.68	2.52	1.71	2.56	1.71	2.57	1.67	2.49	1.68	2.51
250	1.91	2.98	1.91	2.96	1.92	2.97	1.90	2.95	1.93	3.00	1.93	3.00	1.88	2.91	1.90	2.94
300	2.14	3.41	2.13	3.40	2.13	3.39	2.12	3.38	2.16	3.44	2.15	3.43	2.10	3.33	2.11	3.36
350	2.36	3.85	2.35	3.84	2.33	3.81	2.34	3.82	2.37	3.87	2.37	3.87	2.31	3.75	2.33	3.79
400	2.59	4.30	2.58	4.28	2.55	4.24	2.56	4.25	2.60	4.31	2.59	4.30	2.52	4.17	2.54	4.21
450	2.81	4.75	2.80	4.72	2.77	4.67	2.78	4.68	2.81	4.75	2.81	4.74	2.73	4.59	2.76	4.65
500	3.03	--	3.02	--	2.98	--	2.99	--	3.04	--	3.03	--	2.94	--	2.97	--
450	2.81	--	2.80	4.72	2.78	4.68	2.77	4.68	2.82	4.76	2.82	4.76	2.73	4.60	2.76	4.65
400	2.58	4.31	2.58	4.29	2.56	4.25	2.57	4.25	2.60	4.33	2.60	4.32	2.52	4.18	2.55	4.22
350	2.36	3.87	2.36	3.85	2.35	3.83	2.35	3.81	2.38	3.87	2.37	3.89	2.31	3.76	2.33	3.80
300	2.13	3.41	2.14	3.41	2.13	3.40	2.12	3.38	2.17	3.45	2.15	3.44	2.10	3.34	2.11	3.36
250	1.91	2.97	1.91	3.02	1.92	2.97	1.90	2.95	1.94	3.01	1.93	3.01	1.88	2.91	1.89	2.93
200	1.69	2.53	1.69	2.53	1.70	2.55	1.59	2.52	1.72	2.58	1.71	2.57	1.67	2.49	1.68	2.51
150	1.46	2.08	1.47	2.09	1.49	2.13	1.47	2.09	1.50	2.14	1.50	2.14	1.46	2.08	1.46	2.08
100	1.23	1.64	1.25	1.66	1.27	1.71	1.24	1.66	1.28	1.71	1.27	1.71	1.25	1.66	1.24	--
50	1.00	1.19	1.02	1.21	1.05	1.28	1.03	1.23	1.05	1.27	1.05	1.27	1.03	1.23	--	---
0	0.75	0.78	0.80	0.77	0.84	0.86	0.80	0.80	0.82	0.82	0.82	0.83	0.81	0.81	--	--

*Highs and lows in inches of deflection

TABLE V

AVERAGE TRACE DEFLECTIONS FOR H_x AND H_y CHANNELS

H_y lb	High* Average	Low* Average	H_x lb	High Average	Low Average
0	0.805	0.806	0	0.698	0.661
50	1.24	1.03	50	1.15	0.900
100	1.67	1.25	100	1.61	1.13
150	2.11	1.47	150	2.05	1.36
200	2.53	1.69	200	2.50	1.59
250	2.96	1.91	250	2.95	1.81
300	3.39	2.13	300	3.38	2.03
350	3.83	2.35	350	3.82	2.25
400	4.26	2.57	400	4.25	2.47
450	4.68	2.78	450	4.53*	2.69
500	--	3.00	500	--	2.91
450	4.69	2.79	450	4.55*	2.70
400	4.27	2.57	400	4.27	2.48
350	3.84	2.35	350	3.83	2.26
300	3.40	2.13	300	3.39	2.04
250	2.97	1.91	250	2.96	1.82
200	2.54	1.69	200	2.52	1.62
150	2.10	1.48	150	2.06	1.37
100	1.68	1.25	100	1.62	1.13
50	1.21	1.03	50	1.16	0.905
0	0.806	0.809	0	0.700	0.664

*Omitted on plot because of insufficient data

* Lows and highs in inches of deflection

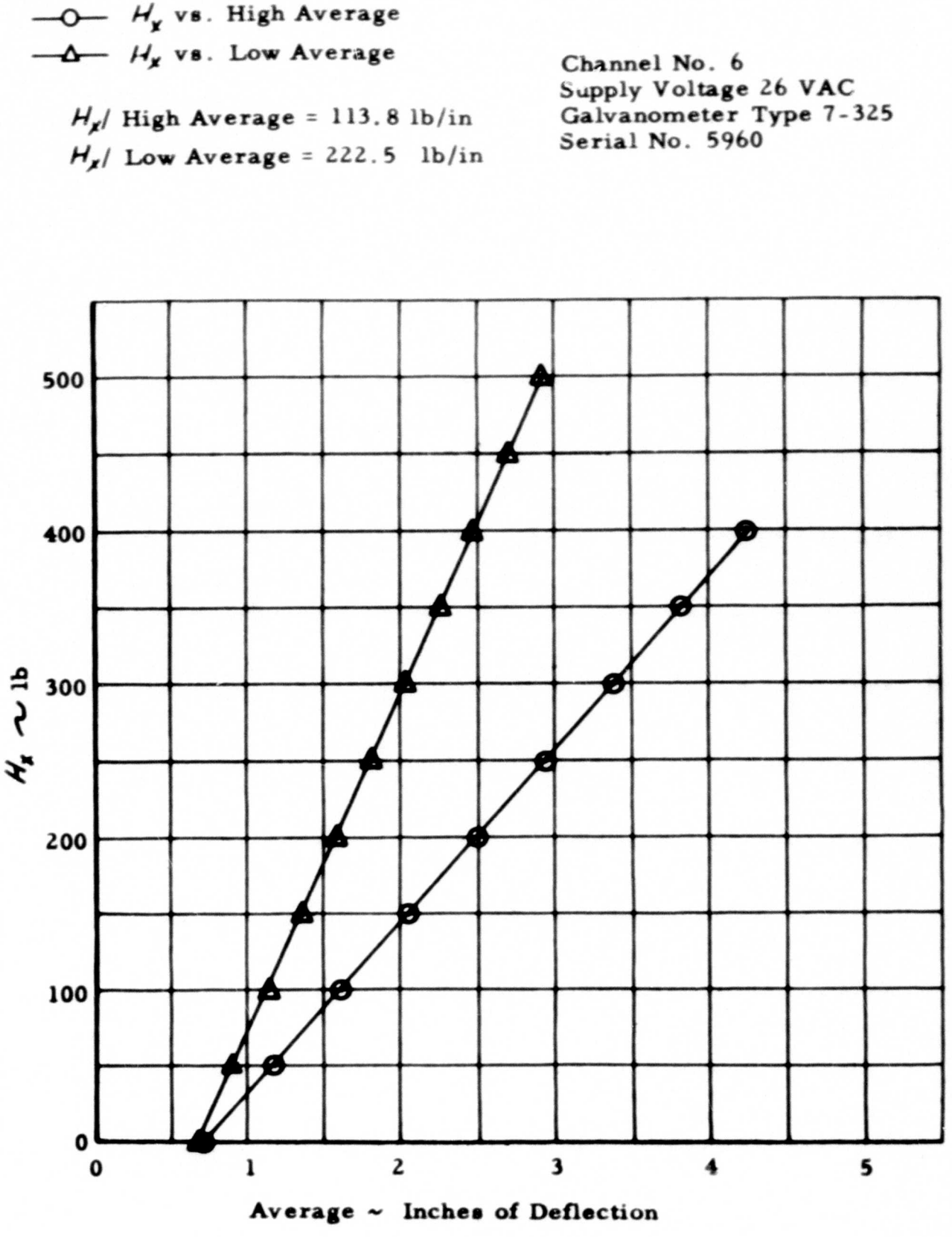

FIGURE 14 H_x CALIBRATION

H_y vs. High Average

H_y vs Low Average

H_y/ High Average = 115.0 lb/in

H_y/ Low Average = 227.5 lb/in

Channel No. 7
Supply Voltage 26 VAC
Galvanometer Type 7-325
Serial No. 5867

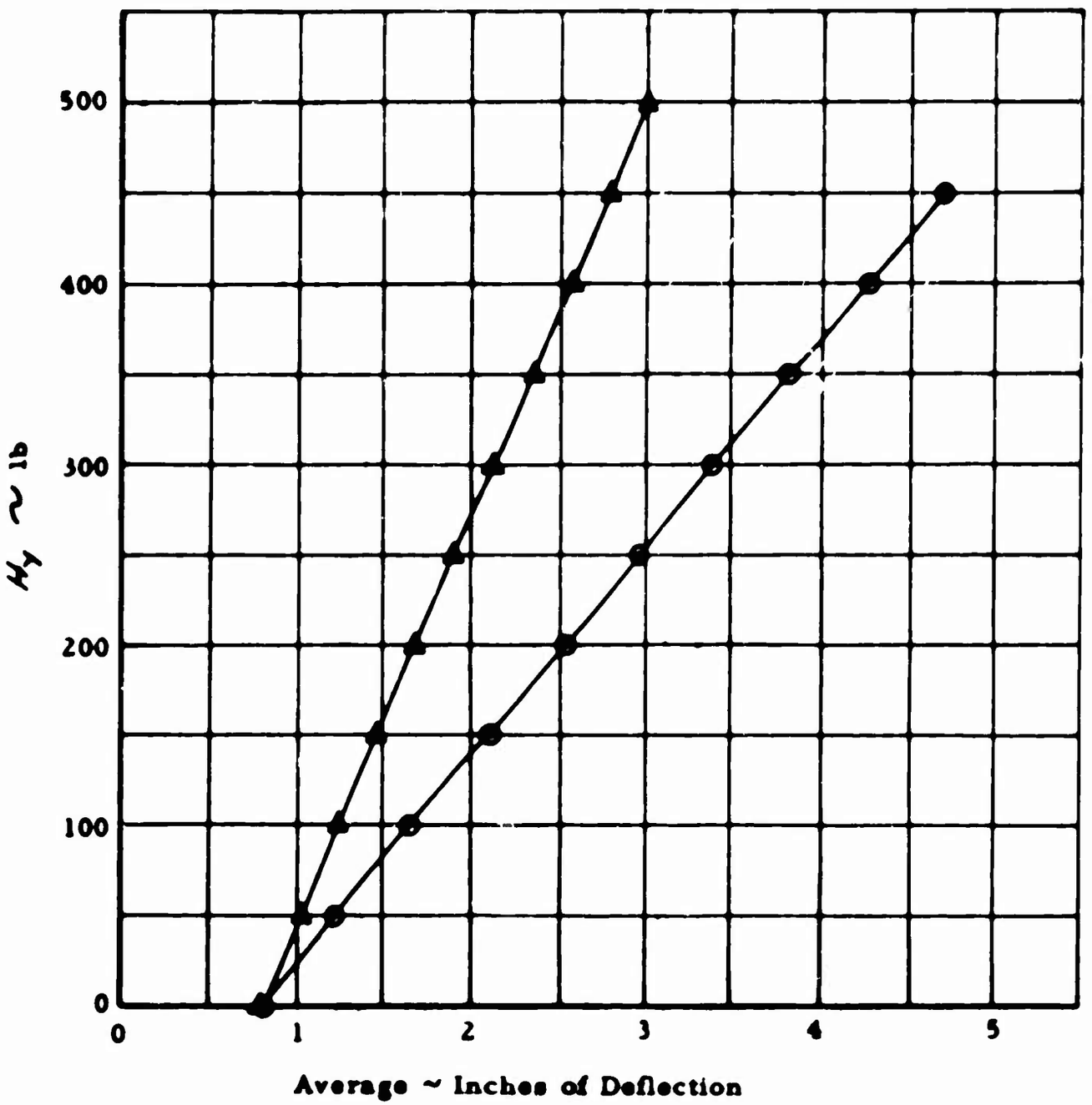

FIGURE 15 H_y CALIBRATION

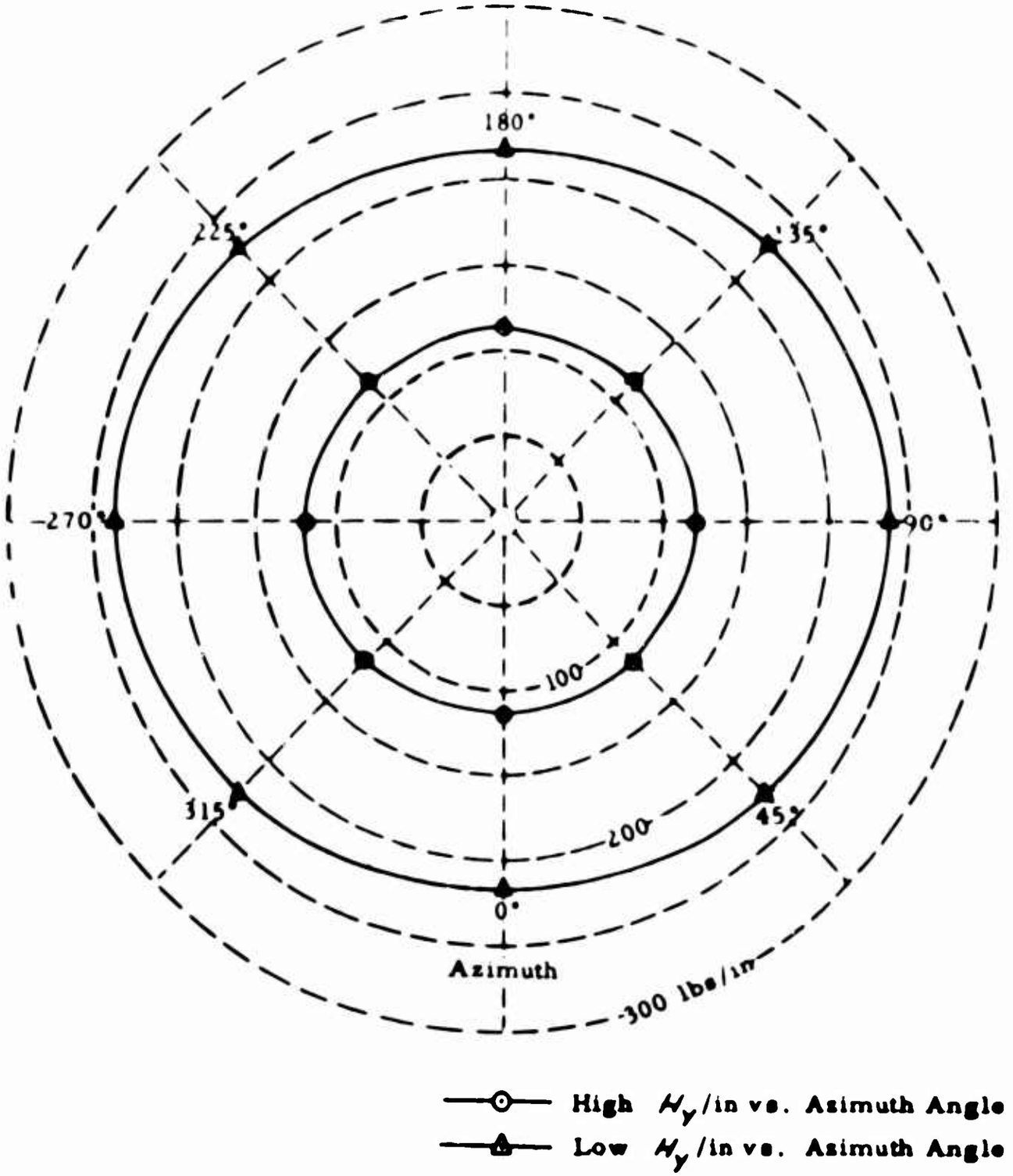

FIGURE 17 H_y CALIBRATION FACTORS AS A FUNCTION OF AZIMUTH

TG-1476-F-1

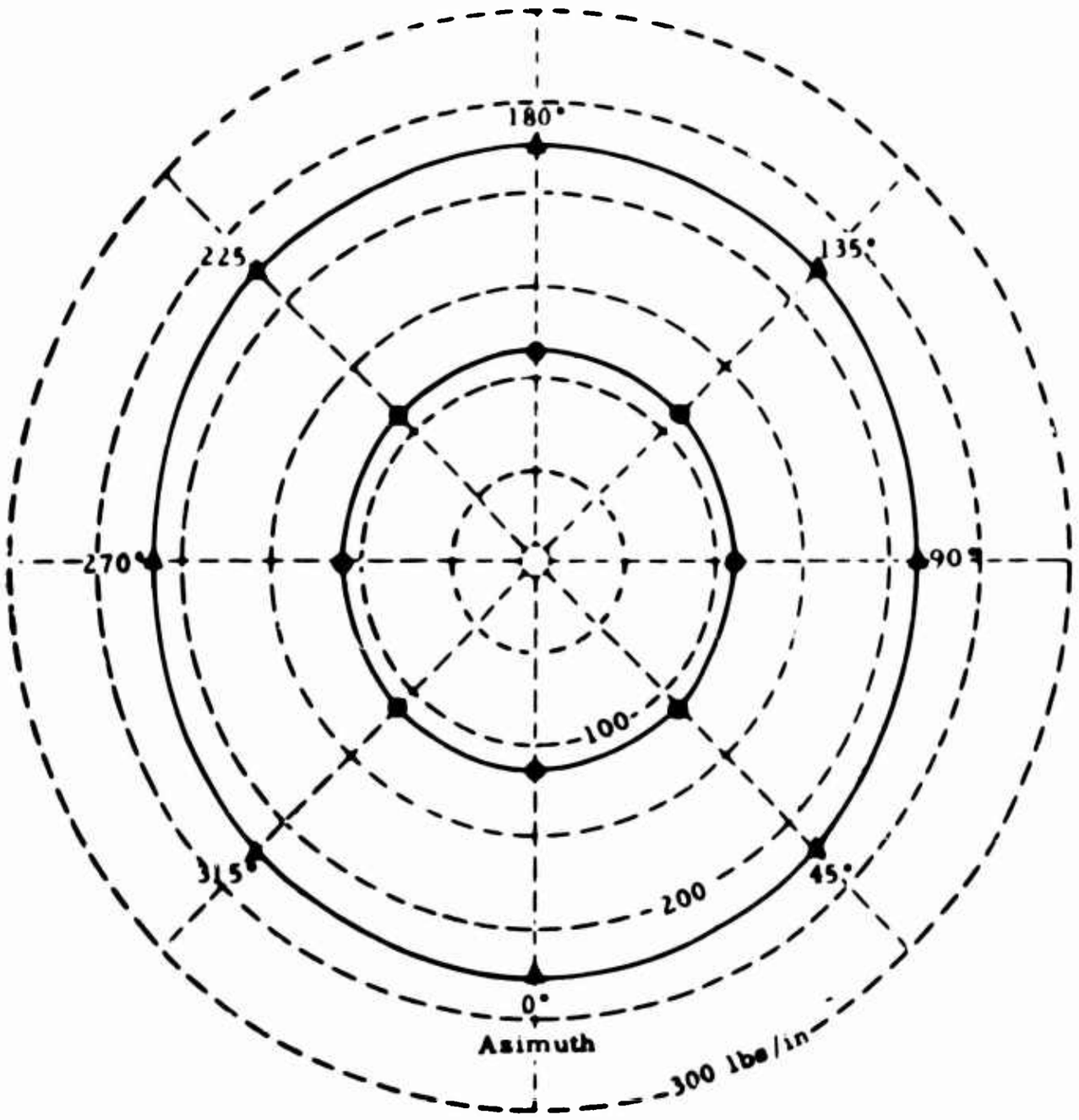

High H_g/in vs. Azimuth Angle

Low H_g/in vs. Azimuth Angle

FIGURE 16 H_g CALIBRATION FACTORS AS A FUNCTION OF AZIMUTH

TG-1476-F-1

BLANK PAGE

SUMMARY AND CONCLUSIONS

The design, construction, and calibration of a shaft force measuring system has been accomplished. The resulting calibrations indicate that the combined errors due to hysteresis, linearity and resolution are less than 1% of full scale for all three force components - H_x , H_y , and T .

The forces measured at the rotor shaft comprise the major portion of the fuselage-rotor interaction forces. The control rods from the swash plate to the blade assembly introduce additional forces which must be added to the shaft tension to obtain the complete axial or rotor lift. The cyclic pitch control input introduces bending moments which are not sensed by the shear bridge arrangement. Since the rotor is a teetering type, it introduces no appreciable bending moment.

A shear component, H_x , will be observed statically because of the 3° tilt of the rotor shaft. For a 5000 lb vertical load, the apparent shear will be approximately 260 lb.

The vector sum of the H and T forces will yield the total rotor-fuselage interaction force and its direction relative to the axis of the rotor shaft.

Provision has been made for switching the filter on and off the tension channel with no gain change. This makes it possible to measure the amplitude of the vertical load fluctuations as well as the more accurate filtered value of the average vertical load.

Careful attention to warm-up and balancing of the signals during operation as well as adjustment of the torque nulling circuit will yield data on the H_x , H_y , and T forces within 1% to 2% accuracy. The system is capable of higher accuracy, but it is doubtful whether the measurements can be made to that accuracy because of the mechanical vibration and other factors which will introduce random errors and fluctuations in the measured data.

BIBLIOGRAPHY

1. Deazley, W. and Schultz, E., The Determination of Helicopter Longitudinal Stability Derivatives from Flight Data. Part I - Development of Flight Test Instrumentation, Techniques and Analysis Methods, Cornell Aeronautical Laboratory Report No. BB-981-F-1, WADC TR 55-438, Part 1, February 1957.

2. Schultz, E., The Determination of Helicopter Longitudinal Stability Derivatives from Flight Data. Part II - Analyses of Flight Data and Extraction of Basic Stability Derivatives, Cornell Aeronautical Laboratory Report No. BB-981-F-2, WADC TR 55-438, Part 2, September 1959.

3. Schultz, E., An Analog Computer Study of Flight Measured Longitudinal Transient Motions of a Single Rotor Helicopter, Cornell Aeronautical Laboratory Report No. TG-1202-F-1, WADC TR 55-438, Part 3, October 1959.

4. Deazley, W. and Schultz, E., Flight Test Determination of Lateral Stability and Control Derivatives for a Single Rotor Helicopter, Part I - Equations of Motion, Analysis Techniques, Instrumentation, and Flight Shakedown, Cornell Aeronautical Laboratory Report No. TB-1288-F-1, WADC TR 59-754, Part 1, July 1959.

5. Chalk, C., Flight Test Determination of Lateral Stability and Control Derivatives for a Single Rotor Helicopter. Part II - Data Flights, Cornell Aeronautical Laboratory Report No. TB-1288-F-2, WADC TR 59-754, Part 2, October 1959.

APPENDIX I

The resolver gearbox designed and constructed at Cornell Aeronautical Laboratory, Inc., was used to convert the shaft rpm of the Tachometer Generator into a shaft output having the exact rpm of the main rotor shaft. This output shaft must also be locked to the main rotor shaft position so that it will never slip out of synchronization with the main rotor shaft. This is essential for the correct resolution of the H_x and H_y forces.

The gear ratio between the Tachometer Generator shaft and the main rotor is

18/19 x 26/27 x 41/55 x 57/176 x 57/176

This can be simplified to

57/176 x 41/176 x 52/55

which is the basis for the gearing employed.

Figure 18 is the assembly drawing of the gearbox.

The actual gearing employed is:

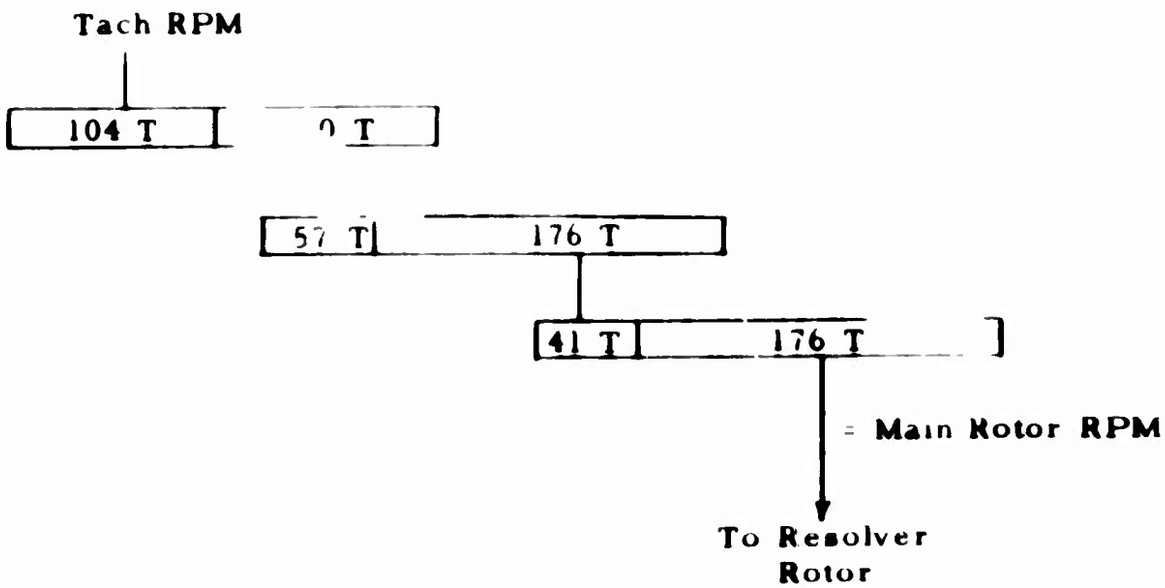

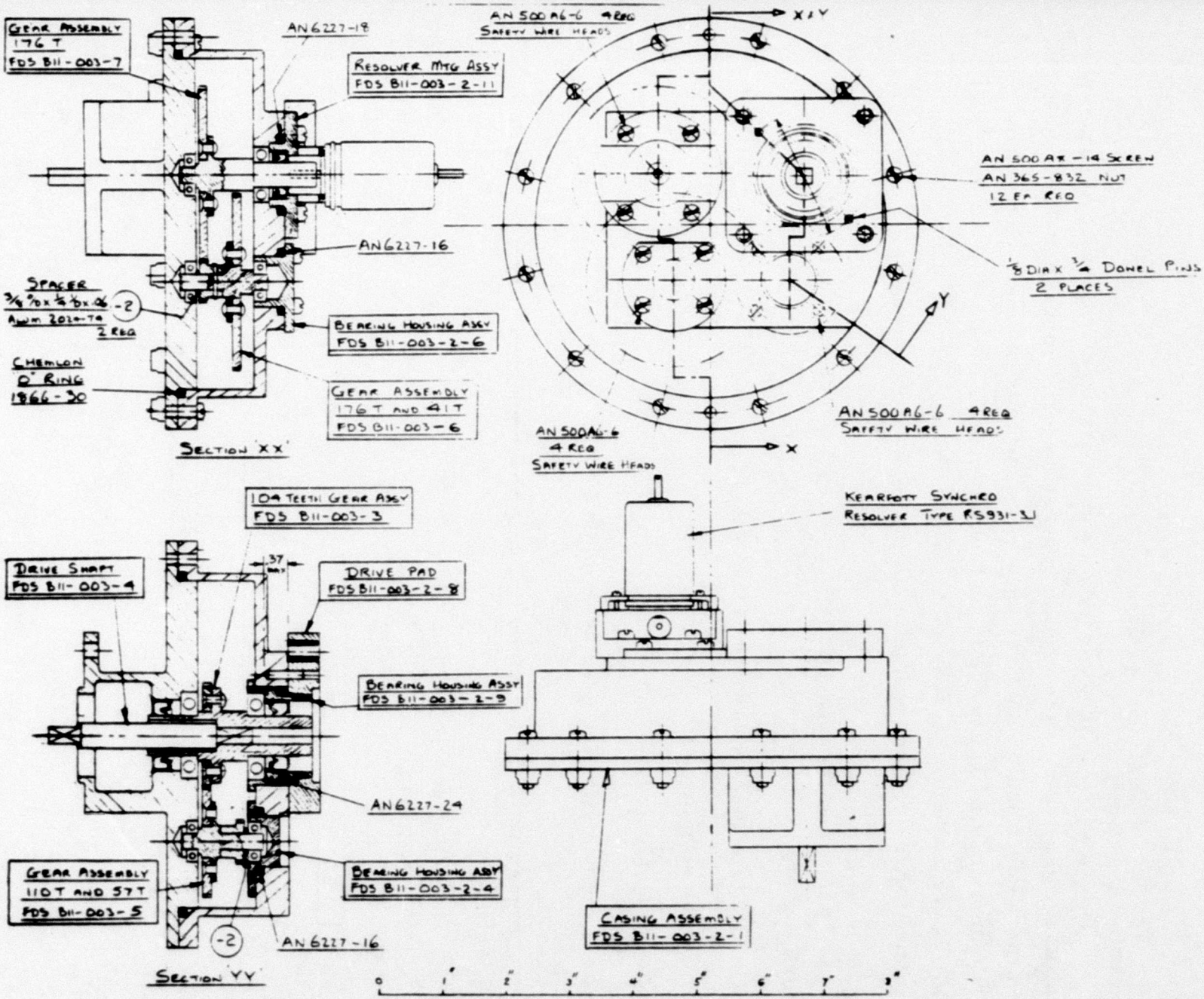

FIGURE 18 ASSEMBLY DRAWING OF THE GEARBOX